

# Advances in actinide thin films: synthesis, properties, and future directions

Kevin D. Vallejo<sup>1,\*</sup>, Firoza Kabir<sup>1,2</sup>, Narayan Poudel<sup>1</sup>, Chris A. Marianetti<sup>3</sup>, David H. Hurley<sup>1</sup>, Paul J. Simmonds<sup>4,5</sup>, Cody A. Dennett<sup>1</sup>, and Krzysztof Gofryk<sup>1,†</sup>

<sup>1</sup>*Condensed Matter and Materials Physics, Idaho National Laboratory, Idaho Falls, ID 83415, USA*

<sup>2</sup>*Glenn T. Seaborg Institute, Idaho National Laboratory, Idaho Falls, ID 83415, USA*

<sup>3</sup>*Department of Applied Physics and Applied Mathematics,  
Columbia University, New York, NY 10027, USA*

<sup>4</sup>*Department of Physics, Boise State University, Boise, ID 83725, USA and*

<sup>5</sup>*Micron School of Materials Science and Engineering, Boise State University, Boise, ID 83725, USA*

(Dated: April 25, 2022)

Actinide-based compounds exhibit unique physics due to the presence of  $5f$  electrons, and serve in many cases as important technological materials. Targeted thin film synthesis of actinide materials has been successful in generating high-purity specimens in which to study individual physical phenomena. These films have enabled the study of the unique electron configuration, strong mass renormalization, and nuclear decay in actinide metals and compounds. The growth of these films, as well as their thermophysical, magnetic, and topological properties, have been studied in a range of chemistries, albeit far fewer than most classes of thin film systems. This relative scarcity is the result of limited source material availability and safety constraints associated with the handling of radioactive materials. Here, we review recent work on the synthesis and characterization of actinide-based thin films in detail, describing both synthesis methods and modelling techniques for these materials. We review reports on pyrometallurgical, solution-based, and vapor deposition methods. We highlight the current state-of-the-art in order to construct a path forward to higher quality actinide thin films and heterostructure devices.

## I. INTRODUCTION

Due to their strong electronic correlations and populations of dual-natured  $5f$  electrons, the actinide elements, with atomic numbers ranging from 89 to 103, represent a rather poorly understood section of the periodic table. These transition elements with partially filled  $5f$  electronic subshells exhibit a wide range of exotic properties. They have multiple oxidation states: in an aqueous solution, Pu can exist in four different states simultaneously, for example. Their  $5f$  electrons can occupy itinerant or highly localized states [1]. They also exhibit divergent magnetic properties, from nearly magnetic (Np and Pu) to transition-metal-like behavior (Th, Pa, U) [2]. Technologically, the most widely used actinide compound to date has been  $\text{UO}_2$ , in its role as the primary fuel for commercial nuclear energy production [3, 4].

Despite these unique physical properties, their scarcity, inherent radioactivity, and challenges concerning their synthesis mean that actinide materials are still some of the least understood elements. Transuranic actinides and their compounds have been confined to specialized facilities where materials control and accountability can be ensured. Their study and understanding are further hindered by their low natural abundance and typically short half-lives, which limit material supply [1]. Developing an understanding of the fundamental properties and performance characteristics of actinide compounds is hence a challenging but highly active area of research [5]. Understanding the physics of these complex materials more deeply will ensure their continued technological relevance, and open new avenues for discovery in the domains of quantum science and strongly correlated sys-

tems.

One way to enable this expansion in our understanding is to minimize the structural complexity in experimental specimens. In practice, this could include removing crystallographic defects, grain boundaries, chemical heterogeneities, and other imperfections during the synthesis process. To this end, thin film synthesis techniques have been used to produce high-quality, single crystalline specimens of various actinide compounds, including those used in nuclear fuel to study their physical properties [6]. Such efforts also aid comparison between experimental measurements and results from modeling and simulation tools. The geometries of these thin-film samples also permit the implementation of “microlaboratory” experimental designs, wherein chemical reactions may be explored in detail [7]. It is important to note that due to their scarcity, reactivity, radioactivity, and toxicity, high-purity actinide samples in *any* geometry have only recently become available to use as targets or sources [8]. However, despite these constraints, researchers have found ways to explore a range of physical, chemical, and solution-based techniques capable of producing actinide-based films with varying degrees of success and quality. Here we catalog the successes, and highlight some of the unique property and performance data generated to date.

This review is organized as follows: in section II we describe the synthesis methods used to create actinide-based thin films. Section III provides a review of actinide thin films that have been successfully synthesized, along with the techniques used for their structural, electronic, and surface characterization. Section IV summarizes the current and theorized properties of actinide thin films,

and in section V we give an overview of the efforts and challenges related to modelling these structures. Finally, in section VI we explore the rich scientific and technological promise of combining different actinide thin films into heterostructures, together with the associated challenges for this next step in the use of these important compounds.

## II. SYNTHESIS METHODS

Ever since the discovery of radiation and its properties, there has been a need to refine and purify actinide materials. During the twentieth century, the focus shifted from Ra to U in the more than 180 minerals containing these elements [9]. Motivated by the applications of radioactive compounds, technology evolved and reports began to emerge of the synthesis of actinide single crystals and thin films. One of the earliest examples is from 1955, when Pu and U were dissolved in a cellulose lacquer and painted on metallic foils [10]. The intervening 70 years have seen synthesis techniques developed that incorporate the refined safety measures necessary to handle these materials.

Spirlet and Voigt summarized the first attempts at refining actinide metals and compounds [8]. Their review article includes the metallothermic reduction of oxides and halides, as well as vacuum melting, selective evaporation and condensation, electrorefining, zone melting, and electrotransport (see [8] and references therein). They highlight solution-based techniques as the most economical approach for single crystal synthesis. In the 40 years since Spirlet and Voigt's review, growth of high quality single crystal actinides has advanced enormously, and these samples are of increasing interest from a fundamental scientific perspective. As safety standards evolve and more institutions have access to actinide sources, here we discuss the different approaches that will be instrumental in helping single-crystal actinides reach their full potential. Figure 1 summarizes several of these techniques including pyrometallurgical, solution-based, and different chemical, physical, and pulsed vapor deposition techniques. Table I also lists these synthesis methods, together with the different compounds they have been used to produce, and substrates when available.

### A. Pyrometallurgical methods

In early attempts to fabricate bulk single crystals, actinide compounds such as oxides or alloys were placed in crucibles. When subjected to extreme temperatures and pressures, the required materials are evaporated from the solid source onto a substrate (Figure 1(a)). The high melting points of actinide and rare-earth materials used in this early attempts presented a challenge for substrate and crucible material selection. Among the first reports attempting to grow actinide thin films was *mineraliza-*

*tion*. In this approach, the crucible is placed on a rotating, water-cooled support, connected to a DC power supply. A tungsten wire acts as a cathode, emitting electrons that weld a lid onto the crucible. Then, by heating the crucible very close to its melting temperature, single crystals can grow inside from the source material over a period of weeks [2, 8, 11]. In this way,  $\text{Ac}_2\text{O}_3$  was chemically converted to a face-centered cubic (fcc) Ac metal powder, along with the presence of actinium hydride discovered through X-ray diffraction (XRD) [12]. Similar approaches have yielded samples of  $\text{Th}_3\text{N}_4$  [13], UN [14],  $\text{U}_2\text{N}_3$  [14], USB [11], UTe [11], and U metal [15]. Different transuranic elements can be synthesized into thin films by reducing their oxide compounds. These materials are loaded into a Ta crucible, together with a reducing agent. The crucible is then heated with direct current filaments in order to evaporate the pure metal and condense it onto a cooler substrate outside of the crucible [15]. Pyrolytic decomposition has been used to thermally break down precursor molecules containing U and Am, and form thin films of these active species [16]. In general, these early methods introduced large numbers of impurities, and resulted in poor control over the crystal quality of each sample. Nonetheless they helped researchers improve their understanding of growth parameters and physical properties, paving the way for more innovative approaches.

### B. Solution-based methods

The levels of radioactivity in some actinide materials make it impractical to handle of more than trace amounts in facilities not designed for this purpose. Dissolving these trace amounts in solution helps minimize the amount of radioactive elements involved in single-crystal growth (Figure 2(b)). One of the most successful approaches to solution deposition to date is polymer assisted deposition (PAD), where precursor molecules are made by binding the metal ions of interest to a polymer. As this polymer solution evaporates, the metal film grows. This technique allows researchers to bypass the need for vacuum equipment by controlling the growth process through the viscosity and homogeneity of the metal-bearing precursor polymers [17–20]. Electrodeposition is another solution-based approach. Atoms of the required metal are suspended in solution and mixed with a metallic stirrer that acts as the anode, while a suitable metal plate onto which the film will grow is kept near the cathode [21–23]. This approach has provided an opportunity to study the oxidation states in uranium oxides [18], and to grow thin films of uranium oxides on foils [24].

Other solution-based approaches include hydrothermal synthesis, in use since 1839 when the first barium and strontium carbonate crystals were formed [25]. Pressure and temperature gradients are used to precipitate the desired material from a high purity feedstock (Figure 2(e)).

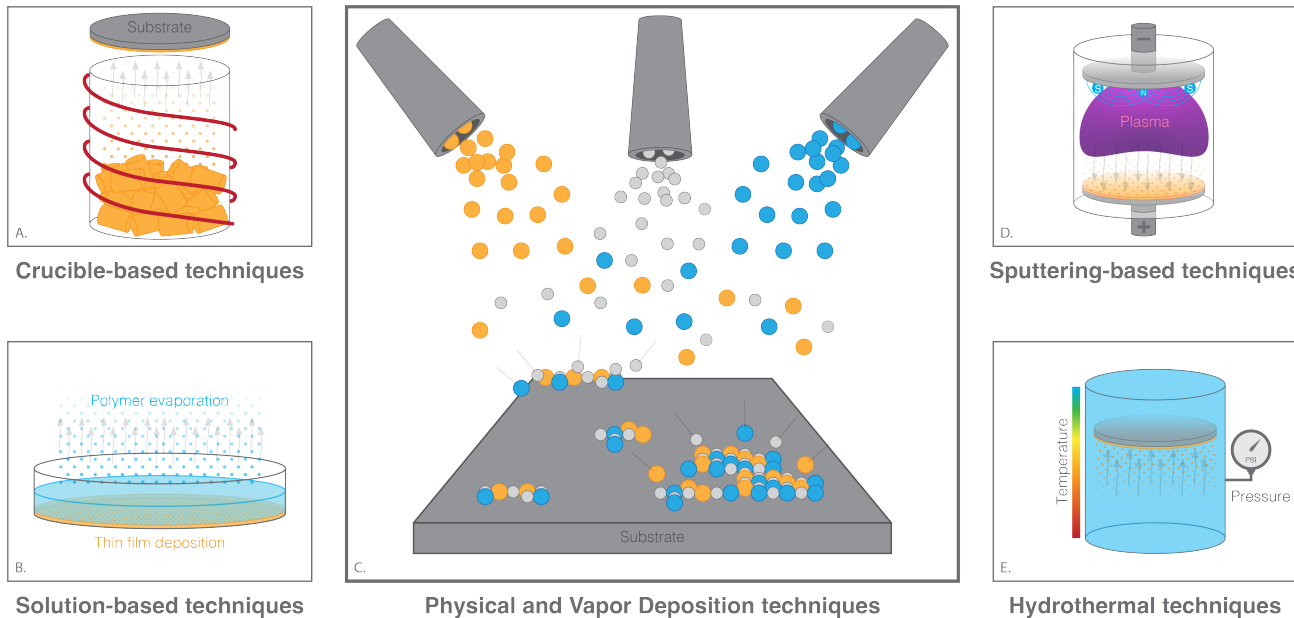


FIG. 1. Schematic representation of the main synthesis techniques used for actinide thin film fabrication. (a) Shows a crucible often used in pyrometallurgical techniques where materials are evaporated from a solid source onto a substrate above. (b) Shows the polymer assisted deposition approach, where as a polymer solution evaporates, the film grows. (c) Depicts a common approach to vapor deposition techniques, where ultra pure material (either in elemental form or in compounds) is directed towards a substrate where it can react with a plasma, other compounds, or simply adsorb on the substrate. (d) Shows a representation of sputtering techniques, where a plasma of ionized material is deposited onto a substrate, with the option to have an overpressure of a different material, such as N or O. (e) Shows the hydrothermal approach, where pressure and temperature gradients are used to precipitate the desired material from a mineralized solution onto a substrate where a thin film can grow.

A mineralized solution (e.g., CsF in the case of  $\text{UO}_2$ ) is often used to help transport the nutrient to the substrate where the thin film can crystallize and grow [26, 27]. The main difference between conventional solution growth and hydrothermal synthesis is the viscosity of the liquid. Several actinide compounds have been successfully synthesized using solution approaches, including  $\text{ThO}_2$  [28, 29],  $\text{UN}_2$  [19],  $\text{UO}_2$  [5, 18, 19, 24, 26, 27, 30],  $\text{U}_3\text{O}_8$  [19],  $\text{UO}_3$  [17],  $\text{UC}_2$  [19],  $\text{NpO}_2$  [19, 20], and  $\text{PuO}_2$  [19].

A key challenge associated with solution-based growth approaches is presence of trace amounts of solvent in the final samples. Although the quality of thin films prepared in the last few years is remarkable, further reductions in defect and impurity densities is still a goal for higher precision measurements.

### C. Physical and chemical vapor deposition methods

Several types of physical vapor deposition (PVD) have been used to synthesize thin films of actinides and sur-

rogate materials (Figure 2(c)). Among these, sputtering and electron beam evaporation (EBE) have been most commonly used due to their comparatively low cost and ease of use. Different types of sputtering are used for the deposition of thin films depending on the physical properties of the targets required: radio frequency (RF), direct current (DC), high frequency (HF), ion beam (IB), and magnetron sputtering are among the most common. Multiple types can be combined to produce enhanced results in terms of faster deposition rates or more uniform films (Figure 2(d)). EBE is commonly used for its ability to heat relatively small areas of a source to very high temperatures, allowing for high precision in deposition rates.

Reactive PVD (RPVD) occurs when a chemical reaction occurs between the deposited material and the atmosphere surrounding the substrate, often during an annealing step. In contrast, pulsed laser deposition (PLD) is a form of physical vapor deposition where a high power, low bandwidth laser is used to melt, evaporate, and ionize material from the surface of a target [3].

Other techniques used mostly for rare-earth com-

pounds include chemical vapor deposition (CVD) [31, 32] and molecular beam epitaxy (MBE) [33, 34]. There have been numerous successful research efforts to use rare-earths as surrogates for actinide materials [35–39]. Similarities in their densities, electronic structure, and high melting temperatures give researchers an opportunity to develop equipment and growth regimes that can be translated from the rare earths to synthesize actinide thin films.

### III. ACTINIDE THIN FILMS AND CHARACTERIZATION

Commercial applications of actinide-based compounds depend on a thorough understanding of their properties. This knowledge in turn helps researchers develop ways to synthesize higher quality samples. The accuracy of current physical property measurements for actinide-based materials are limited by defects such as grain boundaries and impurities in the samples. Initial studies of the properties of these materials used polycrystalline samples or, in the best cases, samples with large single crystal grains. Defects such as grain boundaries act as scattering centers for thermal energy carriers (electrons and phonons). Electron- and phonon-mediated conduction processes dictate a material’s thermal and mechanical properties, and understanding these is vital for their full characterization. By eliminating grain boundaries, high quality, single crystalline samples enable researchers to study these processes in the absence of major scattering mechanisms. In addition, the use of new sample geometries and crystallographic orientations continue to expose novel physics and materials properties. For example, controlling dimensionality and strain in actinide heterojunctions will create an opportunity to explore novel quantum phenomena. Here we discuss the promise, challenges, and possible synthesis routes for actinide-bearing heterostructures exhibiting complex electron correlations for functional and energy materials.

#### A. Thin film synthesis

Thin films of actinium metal have been produced since 1953, while thin films of metallic protactinium were synthesized through electrodeposition as early as 1964 [23]. These metallic thin films were used for  $\alpha$ -spectrometry and nuclear reaction experiments. Following this work, deposition of thin films of protactinium pentoxide ( $\text{Pa}_2\text{O}_5$ ) by electro-spraying films was achieved [22].

Reports of thorium-based thin film properties remain relatively scarce due to the absence of a  $5f$  electron orbital. Instead, most attention has focused on thorium’s bulk properties as a candidate fuel for nuclear reactors. With this objective in mind, films of  $\text{ThO}_2$  have been synthesized using sputtering [40, 41], photochemical de-

position [28], and electron beam evaporation [42]. Uno *et al.* used a nitridation approach to synthesize  $\text{Th}_3\text{N}_4$  [43]. Gouder *et al.* prepared thin films of  $\text{ThN}$  and  $\text{Th}_3\text{N}_4$  using sputter deposition, where photoemission spectroscopy demonstrated a high density of  $6d$  states in  $\text{ThN}$  and a non-metallic character in  $\text{Th}_3\text{N}_4$  [44].

UN thin films have been grown via reactive and DC magnetron sputtering using a Nb buffer layer on the (1 $\bar{1}$ 02) facet of sapphire [45], as well as on Si(111), polycrystalline Ta foil and glass substrates [46]. Black *et al.* used the same set of substrates (Si(111), polycrystalline Ta foil, and glass) in attempts to grow  $\text{U}_2\text{N}_3$  [46]. Scott *et al.* synthesized  $\text{UN}_2$  on LAO(001) substrates using polymer assisted deposition [19]. Long *et al.* also achieved the growth of both of these compounds by nitriding U metal flakes [47]. Gouder *et al.* grew this compound on  $\text{CaF}_2$  using DC magnetron sputtering [48]. Adamska *et al.* grew UMo films on a Nb(110) buffer layer on a sapphire substrate as well as U-Zr, U-Mo, and U-Nb [49]. The study by Black *et al.* also included thin films of  $\text{UC}_2$  grown on YSZ(110) and  $\text{U}_3\text{O}_8$  in different crystal structures that depended on the orientation of the sapphire substrates [46]. Thin films of uranium oxycarbides and oxinitrides were prepared on Si(111) substrates by Eckle and Gouder using reactive DC sputtering [50]. Two compounds of uranium oxide were grown using PAD on LSAT(100) substrates:  $\alpha$ - $\text{UO}_3$  and  $\alpha$ - $\text{U}_3\text{O}_8$  [17].

Several attempts at synthesizing  $\text{UO}_2$  thin films have been reported with various results. The first reported attempt is by Bierlein and Mastel in 1960, where they studied the effects of irradiation by growing  $\text{UO}_2$  on carbon substrates [51]. Elbakhshwan and Heuser summarized the evolution of  $\text{UO}_2$  thin film growth up to 2017 [52], and discusses the use of CVD and sputtering techniques (see Table I). Their contribution also includes growth on several different substrates using magnetron sputtering. Further advances in this field since then include reactive sputtering on LSAT(110) [53, 54], magnetron sputtering on YSZ(100) [55], DC sputtering on  $\text{SrTiO}_3(110)$  [56], PAD of  $\text{UO}_{2+x}$  by Zhang *et al.* [57], and spin coat combustion on aluminum sheets by Roach *et al.* [58].  $\text{U}_x\text{Th}_{1-x}\text{O}_2$  thin film synthesis was achieved by Cakir *et al.* to study surface reduction using ice [59].

Synthesis of transuranic compound thin films has been historically challenging due to the high toxicity and scarcity of material precursors [60]. An early attempt to produce thin films of  $\text{PuO}_2$  is reported by Shaw *et al.* [61]. More recently, Wilkerson *et al.* summarized the state-of-the-art and reported the growth of thin films using PAD on YSZ substrates [62]. Roussel discussed the sputtering of  $\text{PuO}_2$  and  $\alpha$ - $\text{Pu}_2\text{O}_3$  films used to study inverse photoemission [63]. Subsequent attempts to grow bulk single crystals of these oxides used solution based approaches [64–66]. Other Pu-based single crystal compounds synthesized include PuAs, PuSb, and PuBi for studies of anisotropic magnetization [2]. Mannix *et al.* used the same fabrication method to grow NpS and PuSb single crystals to investigate their magnetic struc-

ture [67]. Durakiewicz *et al.* investigated the spectral features of USb, NpSb, PuSb, NpTe and PuTe using angle-resolved photoemission spectroscopy (ARPES) on samples grown using a mineralization technique [11]. Gouder *et al.* grew thin films of PuSe and PuSb for study using ultraviolet photoelectron spectroscopy (UPS) [68], and thin films of PuSi<sub>x</sub> (with  $x$  varying from 4 to 0.5) [48]. A particularly successful research program involved PAD of PuO<sub>2</sub> and NpO<sub>2</sub> with high enough crystalline quality that they enabled studies of band dispersion and the Fermi surface, and helped validate several characteristics used in  $5f$  electron modelling approaches [19]. NpO<sub>2</sub> was grown on LAO(001) substrates using a UO<sub>2</sub> buffer layer. Elements beyond Np have scarcely been fabricated in sufficient amounts to attempt high quality crystal growth. Through a method of oxidation, Radchenko *et al.* managed to fabricate high quality bulk samples of Am, Cm, Bk, and Cf on a La crucible [15].

## B. Characterization of Thin Films

We can divide materials characterization techniques into categories that deal with different properties of the thin films in question. Figure 2 illustrates how one can use various techniques to explore structural, surface and electronic properties together in concert.

We can obtain plan view or cross-sectional structural images of a thin film using transmission electron microscopy (TEM), scanning electron microscopy (SEM) (see Figure 2(c) and (h)), atomic force microscopy (AFM), and scanning tunneling microscopy (STM). These can be used to determine the size of crystallites, the density of defects such as dislocations twins and stacking faults, and crystalline quality, in addition to quantifying the roughness of the surfaces and the shape, size and areal density of any structures present on them. “Indirect” structural characterization may include Rutherford back scattering (RBS), XRD, and Raman spectroscopy (see Figure 2(a), (d), (e), (f), (i), and (k)). These techniques can provide information that complements what can be seen in microscopy, and help identify properties such as alloy composition, lattice parameter, and in the case of ion-damaged samples, penetration depth.

Several techniques have been used to measure the thermophysical properties of bulk actinide materials [4]. However, thin films have been targeted in specific cases as a means to increase measurement accuracy while using non-destructive techniques. It is here where photothermal approaches offer a viable option for studying samples with small physical dimensions without damage to the sample or the need for destructive sample preparation approaches [95]. Several comprehensive reviews have been recently published on the thermophysical properties of actinide oxides [4], nitrides [96], and carbides [97, 98] due to the importance of these compounds to nuclear science and industry.

Electronic structure characterization includes angle-resolved photoemission spectroscopy (ARPES), X-ray photoemission spectroscopy (XPS), STM-based scanning tunneling spectroscopy (STS), and photoluminescence spectroscopy. These approaches can shed light on charge carrier behavior, and the electronic states present in a given material. These characteristics are of particular interest for actinide thin films due to the interesting physics governed by their  $5f$  electron states. XPS allows one to determine the elements present within a material, along with their oxidation and bonding state. XPS is especially useful for samples with reduced dimensionality within which the localization of  $5f$  electrons occurs [99]. Gouder and Havela identified the complications of applying XPS to the study of actinides: an asymmetrical tail in metallic systems can often prove difficult to differentiate from scattering of electrons onto the Fermi level. In addition, the anisotropic distribution of atoms at different temperatures contributes to higher noise levels in the XPS signal [99]. The team lead by Black *et al.* identified the  $5f$  states of UN around 0.8 eV [46]. Havela *et al.* indicate that  $5f$  localization behavior can be studied in PuSb (localized), PuSe (intermediately localized), and PuN (potentially delocalized) [86]. In addition, Gouder *et al.* studied the localization of  $5f$  electrons in PuSi<sub>x</sub> [80]. Durakiewicz *et al.* investigated the systematic changes in the  $5f$  binding energy peak between antimonide and tellurides of U, Pu, and Np [11]. Joyce *et al.* studied the dual nature of  $5f$  electrons using photoemission of  $\delta$ -Pu, PuIn<sub>3</sub>, and PuCoGa<sub>5</sub> [100, 101]. On the same line, Eloirdi *et al.* reported results from XPS studies of PuCoGa<sub>5</sub> deposited using sputtering [102]. Long *et al.* studied the electronic structure of  $\alpha$ -U<sub>2</sub>N<sub>3</sub> and found hints of metallic bonding [73]. Pentavalent uranium was found in U<sub>2</sub>O<sub>5</sub> by Gouder *et al.* using photoemission studies [103].

The ARPES technique has been used to determine precise band structures and Fermi surfaces of actinide-based single crystals [19, 88, 104–127]. Largely focused on bulk actinide compounds, these ARPES studies have created new opportunities for determining the origin of the unusual physical properties of  $5f$ -electron materials. Going forward, ARPES-based studies of epitaxial actinide thin films could lead to the discovery of a wide range of emerging electronic, magnetic, and structural phenomena (Figure 2(j)). Interactions between the epitaxial thin film and the underlying substrate can produce properties that are substantially different from those of the bulk materials. For instance, it has been reported that one can obtain an unusual hexagonal close-packed phase of uranium (hcp-U) by depositing U thin films onto a W (110) substrate [128, 129]. Theoretical calculations predict that the hcp-U phase has an electronic instability, that could lead to a possible charge density wave or magnetic ordering [130]. Different orientations of the  $\alpha$ -U orthorhombic phase can also be obtained by depositing U onto a variety of buffer/seed layers on sapphire substrates [82, 131]. ARPES was used to obtain the band structure of  $\alpha$ -U

TABLE I. Actinide thin film material growth summary.

Compound	Growth Method	Buffer Layer(s) - Substrate	Reference
Ac/AcH <sub>2</sub>	Solid reaction		[12]
Pa	Solution	Zn, Al, Mn	[1]
ThO <sub>2</sub>	RF sputtering	various	[40]
	RF sputtering	glass/Si	[41]
	Photochemical deposition	polyimide membrane	[28]
	EBE	poly-Ir	[42]
	Hydrothermal		[29]
ThN	metal reaction	N/A	[13]
	DC sputtering	quartz	[44]
Th <sub>3</sub> N <sub>4</sub>	Nitridation	N/A	[43]
	DC sputtering	Si(111)	[44]
UN	Reactive sputtering	Si(111) poly-Ta foil glass	[46]
	DC magnetron sputtering	$\langle 011 \rangle_{\text{Nb}} \parallel \langle 1\bar{1}02 \rangle_{\text{Al}_2\text{O}_3}$	[45]
	Reactive sputtering	Spectrosil quartz glass	[69]
	DC sputtering	quartz glass	[70]
	Cathode sputtering	Niobium	[71]
	Nitridation		[14]
UN <sub>1.85</sub>	RF sputtering	Si	[72]
$\alpha$ -U <sub>2</sub> N <sub>3</sub>	Nitridation		[14]
$\beta$ -U <sub>2</sub> N <sub>3</sub>	Cathode sputtering	Si(100)	[73]
	Nitridation		[14]
U <sub>2</sub> N <sub>3</sub>	Reactive sputtering	Si(111) poly-Ta foil glass	[46]
	DC magnetron sputtering	CaF <sub>2</sub>	[45]
UN <sub>2</sub>	PAD	$\langle 111 \rangle_{\text{UN}_2} \parallel \langle 001 \rangle_{\text{LAO}}$	[19]
UO <sub>2</sub>	Reactive sputtering	LAO (001) / CaF <sub>2</sub> (100)	[74]
	Reactive sputtering	$\langle 001 \rangle_{\text{UO}_2} \parallel \langle 011 \rangle_{\text{LSAT}}$	[53, 75]
	Magnetron sputtering	$\langle 001 \rangle_{\text{UO}_2} \parallel \langle 001 \rangle_{\text{YSZ}}$	[54]
	Magnetron sputtering	$\langle 111 \rangle_{\text{UO}_2} \parallel \langle 111 \rangle_{\text{Si}}$	[76]
	Sputtering	Mo	[77]
	Chemical vapor deposition	UO <sub>2</sub> on Si	[32]
	Pulsed laser deposition	$\langle 100 \rangle_{\text{UO}_2} \parallel \langle 111 \rangle_{\text{LSAT}}$	[3]
	PAD	$\langle 001 \rangle_{\text{UO}_2} \parallel \langle 011 \rangle_{\text{LAO}}$	[18, 19]
	sol-gel	MgO, Al <sub>2</sub> O <sub>3</sub>	[78]
	Solution/foil	Fe	[24]
	Solution Spin Coat	Al	[30]
	DC sputtering	$\langle 001 \rangle_{\text{UO}_2} \parallel \langle 011 \rangle_{\text{SrTiO}_3}$	[55]
	DC sputtering	$\langle 111 \rangle_{\text{UO}_2} \parallel \langle 111 \rangle_{\text{YSZ}}$	[56]

single crystals at 173 K [132]. The valence band structure of  $\alpha$ -U was studied in details using ultraviolet photoemission spectroscopy and X-ray photoemission spectroscopy [133],

For ordered overlayers of U metal grown on a W (110) substrate, band-like properties of the U 5*f* states were observed, which were proposed to arise from direct *f*-*f* electron interactions [128]. STM/STS results showed that the U density of states close to the Fermi level is dominated by the 5*f* states [129]. STS and ARPES showed both the Fermi surface topology and electronic structure of ordered  $\alpha$ -U films [134]. ARPES studies of epitaxial thin films of the oxides PuO<sub>2</sub> and NpO<sub>2</sub> [20, 135], and uranium carbide (UC<sub>2</sub>), reveal the importance of the underlying substrate structure in stabilizing the epitaxial film [136]. But in general, compared

with bulk actinide crystals, only a few ARPES studies have been performed on actinide thin films. Therefore, the use of ARPES to measure novel actinide thin films synthesized with higher quality will produce results that are critical to understanding their reactivity, aging, nuclear fuel behavior, and environmental fate, as well as the potentially rich physics of these exotic 5*f* materials.

TABLE II. Actinide thin film material growth summary (cont.)

Compound	Growth Method	Buffer Layer(s) - Substrate	Reference
UO <sub>2</sub>	Hydrothermal	CaF <sub>2</sub>	[26, 27]
	Hydrothermal	CaF <sub>2</sub> , ThO <sub>2</sub> , UO <sub>2</sub> , YSZ	[5]
	CVD	Si	[31]
	Reactive Magnetron Sputtering	TiO <sub>2</sub> , Al <sub>2</sub> O <sub>3</sub> , YSZ, ZnO, NdGaO <sub>3</sub>	[52]
	PAD	Si	[57]
	Spin coat combustion	Al sheet	[58]
U-O-Pd	Sputter co-deposition	Si	[79]
U <sub>3</sub> O <sub>8</sub> (P62m)	PAD	Al <sub>2</sub> O <sub>3</sub> (001)	[19]
U <sub>3</sub> O <sub>8</sub> (Cmmm)	PAD	Al <sub>2</sub> O <sub>3</sub> (012)	[19]
α-UO <sub>3</sub>	PAD	LSAT(100)	[17]
α-U <sub>3</sub> O <sub>8</sub>	PAD	LSAT(100)	[17]
UC <sub>x</sub> O <sub>y</sub>	Reactive DC sputtering	Si(111)	[50]
UO <sub>x</sub> N <sub>y</sub>	Reactive DC sputtering	Si(111)	[50]
U <sub>3</sub>	DC sputtering	Si(111)	[80]
U <sub>1-x</sub> Mo <sub>x</sub>	DC magnetron sputtering	Nb(110)/Al <sub>2</sub> O <sub>3</sub> (1120)	[81]
UMo	DC magnetron sputtering	Nb(110)/Al <sub>2</sub> O <sub>3</sub> (110)	[49]
USb	Mineralization	N/A	[11]
UTe	Mineralization	N/A	[11]
UC <sub>2</sub>	PAD	⟨001⟩ <sub>UC<sub>2</sub></sub>    ⟨011⟩ <sub>YSZ</sub>	[19]
U	Diode sputtering	poly-Al and Mg	[48]
	Oxide reduction	La crucible	[15]
	UHV Magnetron sputtering	⟨001⟩ <sub>U</sub>    ⟨011⟩ <sub>Nb/W</sub>    ⟨1102⟩ <sub>Al<sub>2</sub>O<sub>3</sub></sub>	[82, 83]
	Sputtering	Al and Mg	[6]
UH <sub>2</sub>	Reactive sputtering	Si (001)	[84]
U <sub>x</sub> Th <sub>1-x</sub> O <sub>2</sub>	DC sputtering	Si(111)	[59]
(U <sub>x</sub> Pu <sub>1-x</sub> )O <sub>2</sub>	DC sputtering	Si(111)	[59]
NpH <sub>2</sub>	Solid-gas reaction		[85]
NpSb	Mineralization	N/A	[11]
NpTe	Mineralization	N/A	[11]
NpO <sub>2</sub>	PAD	UO <sub>2</sub> /LAO(001)	[19]
	PAD	YSZ(100)	[19, 20]
	DC sputtering	Si(111)	[59]
NpS	Mineralization	N/A	[67]
PuN	Reactive Sputtering	Si(111)	[86]
PuH <sub>2</sub> /PuD <sub>2</sub>	Solid-gas reaction		[87]
PuSb	Mineralization	N/A	[2, 67]
PuAs	Mineralization	N/A	[2]
PuBi	Mineralization	N/A	[2]
PuCoGa <sub>5</sub>	Flux growth	not specified	[88]
PuSb	Mineralization	N/A	[11]
PuTe	Mineralization	N/A	[11]

#### IV. THERMOPHYSICAL, MAGNETIC, AND TOPOLOGICAL PROPERTIES OF ACTINIDE THIN FILMS

##### A. Thermophysical Properties

Thermophysical properties play a central role in determining the characteristics of actinide materials. Atomic structure dictates macroscopic behavior, and it is hence important to understand the temperature dependence of these properties. A key research driver in actinide compounds is the qualification process for nuclear fuel materials. This process is heavily reliant on characterizing thermophysical properties: heat capacity, thermal conductivity, elastic constants, and thermal expansion

[4, 137]. Heat capacity has been measured in several important actinide dioxides, such as ThO<sub>2</sub> [95], UO<sub>2</sub> [138], NpO<sub>2</sub> [139], PuO<sub>2</sub> [140]. UO<sub>2</sub> and NpO<sub>2</sub> show an interesting magnetic alignment transition that creates anomalies in their heat capacity. Thermal conductivities have been measured for ThO<sub>2</sub> [141], UO<sub>2</sub> [142], NpO<sub>2</sub> [143], and PuO<sub>2</sub> [144]. The heat capacities of select actinide nitride systems have been measured, including ThN [145], and more recently for the UN-ThN mixtures used in nuclear fuels [96].

Among these properties, thermal diffusivity and conductivity have been recently studied as important factors in determining the properties of a nuclear fuel candidate material [4]. The qualification process requires that intrinsic thermophysical properties be re-

TABLE III. Actinide thin film material growth summary.

Compound	Growth Method	Buffer Layer(s) - Substrate	Reference
PuO <sub>2</sub>	DC sputtering	Si (111)	[89]
	PAD	YSZ(100)	[19, 20, 62]
	Sputtering	$\alpha$ -Pu	[63]
$\alpha$ -Pu <sub>2</sub> O <sub>3</sub>	Sputtering	$\alpha$ -Pu	[63]
PuSi <sub>x</sub>	DC sputtering	Mo (100)	[68]
Am	DC Sputtering	Mo(100)	[90]
AmN	DC Sputtering	Mo(100)	[90]
Am <sub>2</sub> O <sub>3</sub>	DC Sputtering	Mo(100)	[90]
AmO <sub>2</sub>	DC Sputtering	Mo(100)	[90]
AmSb	DC Sputtering	Mo(100)	[90]
Am <sub>2</sub>	Solid-gas reaction		[91]
Am	Oxide reduction	La crucible	[15]
CmH <sub>2</sub>	Solid-gas reaction		[92]
Cm	Oxide reduction	La crucible	[15]
Bk	Oxide reduction	La crucible	[15]
Cf	Oxide reduction	La crucible	[15]

solved independently of any particular specimen geometry, without the competing influence of lattice defects or other chemical or structural imperfections. Building a fundamental understanding of intrinsic properties allows for the effects of these additional complexities, for example the types of structural defects generated under exposure to irradiation, to be systematically included in computational frameworks for engineering-scale performance. Much success to date has been found in the use of non-destructive photothermal techniques to measure these intrinsic thermophysical properties [95]. Such methods broadly consider microscale thermal and acoustic wave propagation, which can be measured via surface deformation, refractive index gradient, acoustic expansion/contraction, or changes in optical reflectivity (thermoreflectance). This last approach can be further subdivided into frequency-domain thermoreflectance, time-domain thermoreflectance, spatial-domain thermoreflectance, and hybrid methods [137, 146]. With small sampling volumes, these methods are broadly applicable to the study of thin films [147]. Although they have not yet been applied to actinide thin films, we anticipate that these techniques will help to shed light on their thermophysical properties in the future.

Heterostructure devices that integrate different functional layers can encounter performance issues as a result of restricted heat dissipation across the heterointerfaces (Kapitza resistance). This restriction in heat dissipation correlates with factors such as interfacial roughness, disorder, dislocations, and bonding. As a result, computational modelling of these interfaces often fails to capture all of their vibrational properties, for example changes in mass density, phonon mean free path, and carrier scattering across the interface [148].

## B. Magnetic properties

Different aspects of electron and phonon behavior have been carefully studied under the influence of magnetic fields. Among these, transport and its different manifestations enabled the observations of several noteworthy phenomena. These physical properties are part of what makes actinides interesting to researchers beyond their nuclear applications [149]. Most transition metal elements have itinerant  $d$  electrons, while lanthanide elements exhibit mostly localized  $4f$  electrons. These facts help us distinguish characteristics related to the conduction band of a material and its magnetic properties relating to the  $4f$  electrons [149]. Due to the scarcity and high cost of <sup>227</sup>Ac, single crystal samples of this metal have been synthesized to date, making it difficult to study its magnetic properties experimentally [150]. A similar situation exists for the actinide elements after Californium.

Considering the intervening elements, Th is a paramagnetic metal with three phases that are heavily influenced by the concentration of impurities present [1]. Pa metal was synthesized relatively early on in the development of actinide research, and it was hence possible to determine its phase transition and superconducting behavior [1], as discussed below. The early actinide metals (U, Np, Pu) show no sign of magnetic ordering mostly because the bandwidth of the  $5f$  electrons in these elements is too wide to satisfy the Stoner criterion [151]. U metal exhibits a weak Pauli-type paramagnetism, with  $\alpha$ -U having a charge-density-wave anomaly around 43 K that has been observed in magnetic susceptibility measurements [1]. Np exhibits spin-orbit coupling in the same order as other crystal-related electric effects, leading to its metallic form and paramagnetic behavior [1]. Elemental Pu can be found in both  $\alpha$ - and  $\delta$ -Pu phases. Recent studies point to a lack of evidence favoring any ordered or disordered magnetism in  $\delta$ -Pu [152], which preferentially forms a valence fluctuation ground state [153].



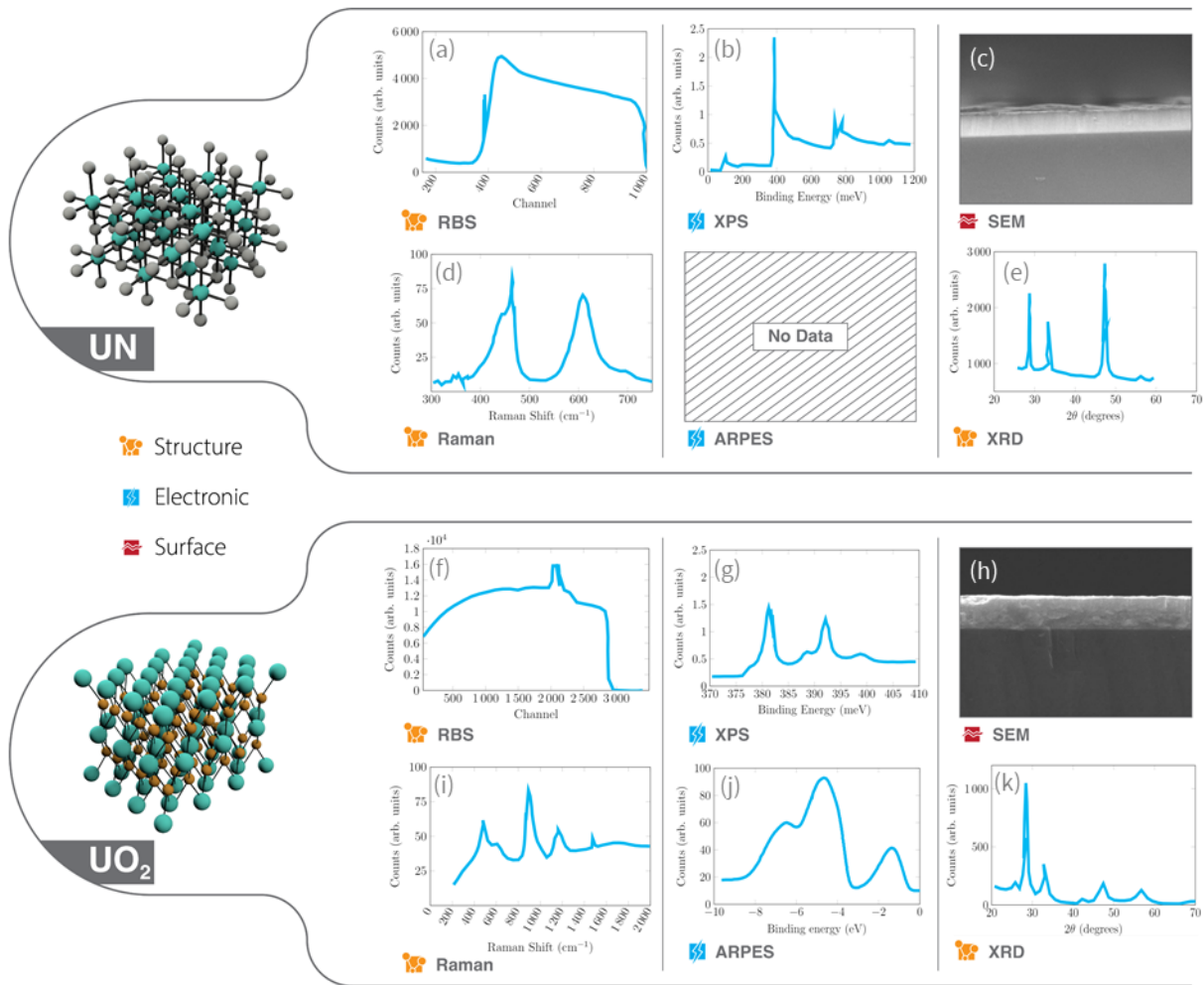


FIG. 2. Characterization techniques applied to the most commonly studied actinide thin films: UN and UO<sub>2</sub>. The data presented in each panel have been digitally extracted from the relevant references and are shown for illustrative purposes only. (a) RBS data from UN before and after radiation exposure ([70]), (b) XPS data for a UN thin film ([45]), (c) SEM micrograph of a UN thin film ([71]), (d) UN Raman spectrum [72], and (e) an XRD diffraction pattern for UN [93]. The equivalent data for UO<sub>2</sub> come from (f) [94], (g) and (h) [76], (i) [3], (j) [19], and (k) from [76]. Note that ARPES data do not yet exist for UN thin films, making initial electronic characterization a near-term target for any new synthesis.

Curium (Cm) is the first element in the actinide series that orders magnetically. Cm is antiferromagnetic (AF) below 65 K in the double hexagonal close packed (dhcp) phase, while in the fcc phase it is ferromagnetic (FM) below 205 K [154]. Berkelium (Bk) also exists in these two crystallographic phases (dhcp and fcc) and similarly orders either AF or FM. Californium (Cf) also exhibits a large effective magnetic moment, similar to Cm and Bk, and likely has a FM ground state [155].

A variety of thin films of actinide compounds have provided insight into the magnetic properties of these systems, such as the magnetic structures of NpS and PuSb [67], itinerant antiferromagnetism [69] and magneto-optical Kerr effect [156] in UN, weak ferromagnetism [157] and antiferromagnetism [74] of UO<sub>2</sub>, and the high

pressure behavior of electrical resistance in NpAs and NpBi [158]. Magnetic susceptibility measurements of transplutonium elements Am, Cm, and Bk helped determine the effective magnetic moments and Curie-Weiss constants for some of their compounds [159]. Magnetic properties have also been extensively studied in these materials using computational methods ([160] and references therein). Bright *et al.* studied the magnetic and electronic structure of UN and U<sub>2</sub>N<sub>3</sub> epitaxial films using x-ray scattering [161]. Recently, using high-field magnetization and magnetostriction measurements, the presence of a metamagnetic transition and a tri-critical point was observed in UN single crystals, leading to the development of a magnetic phase diagram for this material [162, 163]. Using micro-structured single crystals,

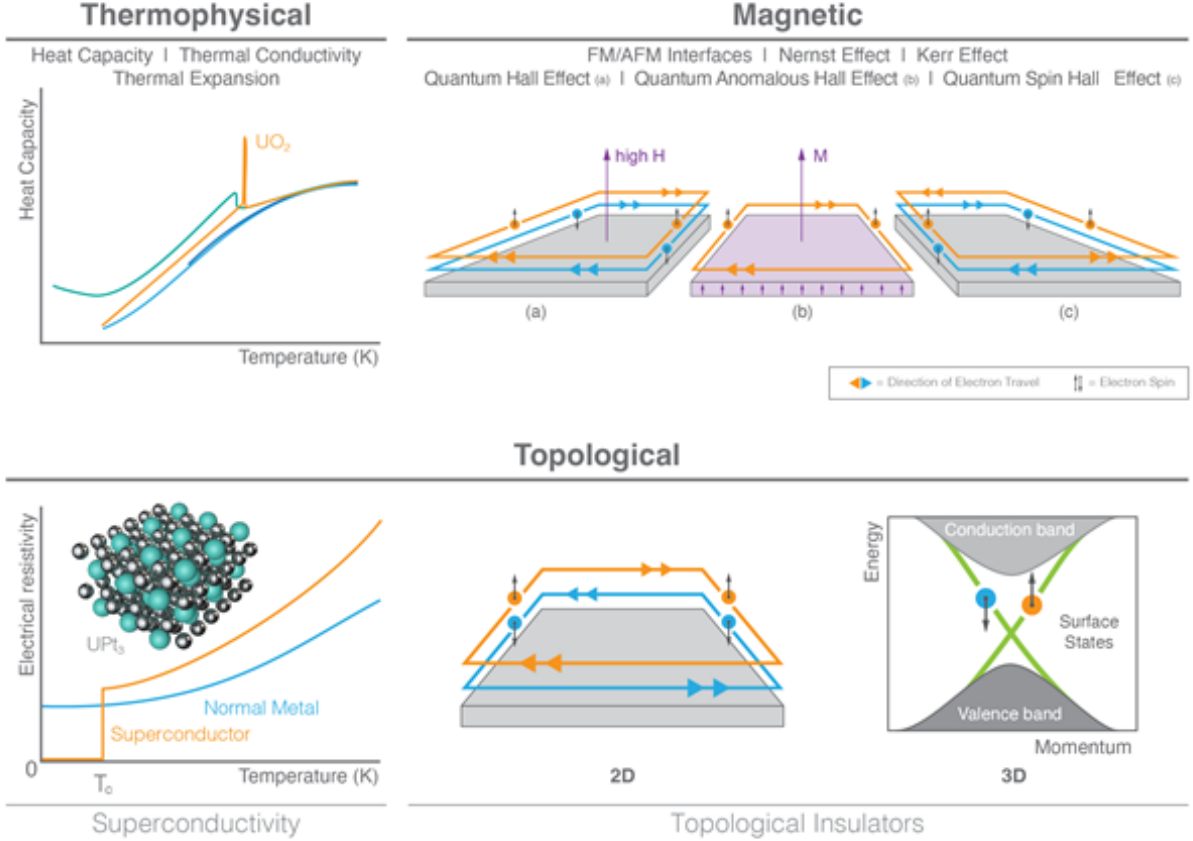


FIG. 3. Properties of interest in select actinide thin films considered in this review. Under thermophysical properties, measurements of heat capacity in some actinide oxides exhibit an anomaly at certain phase transition temperatures. Magnetic properties to consider include the quantum, quantum anomalous, and quantum spin Hall effects. Two important topological properties are superconductivity (present in the  $\text{UPt}_3$  compound, and topologically protected states) together with topological insulators in two and three dimensions, respectively.

Hamann *et al.* found strong reconstruction of the Fermi surface at the high-field transition [164].

### C. Superconductivity

Certain actinide metals are known to exhibit superconductivity at low temperature. These include Th at 1.4 K [165, 166], Pa at 1.4 K [167],  $\alpha$ -U at 0.7 K and  $\gamma$ -U at 1.8 K [168–171]. Am was predicted to be a superconductor, although confirming this experimentally was a challenge due to its large self-heating, scarcity, and radioactivity. However, this prediction was confirmed by Smith and Haire; when its fcc phase is stabilized by quenching, Am becomes superconducting at 1 K [172].  $\alpha$ -Np and  $\alpha$ -Pu have no reported superconducting signature down to 0.5 K [173] and Cm, Bk, and Cf are not expected to show superconductivity because of their magnetic ground-state [173]. There are several

actinide compounds that show heavy-fermion superconductivity, including  $\text{UBe}_{13}$ ,  $\text{UPt}_3$ ,  $\text{URu}_2\text{Si}_2$ ,  $\text{UNi}_2\text{Al}_3$ ,  $\text{UPd}_2\text{Al}_3$ ,  $\text{NpPd}_5\text{Al}_2$ ,  $\text{PuCoIn}_5$ ,  $\text{PuRhGa}_5$ ,  $\text{PuRhIn}_5$  and  $\text{PuCoGa}_5$  [88, 174–179]. Ott *et al.* showed that  $\text{UB}_{13}$  is superconducting below 0.85 K [180]. Joyce *et al.* studied photoemission data from  $\text{PuCoGa}_5$ ,  $\text{PuIn}_3$ , and  $\delta$ -Pu metal. A comparison between their results and model studies indicate characteristics of both itinerant and localized Pu  $5f$  electrons [100]. Furthermore, Joyce compared  $T_c$  in  $\text{PuCoGa}_5$  against  $\text{UCoGa}_5$  and found no evident characteristics of strongly correlated electrons [101]. Thus, valence fluctuations have been proposed as an alternative mechanism for the high-temperature superconductivity observed in  $\text{PuCoGa}_5$  [181, 182]. Recently, unconventional [183], spin-triplet [184] superconductivity with multiple superconducting phases [185] has been reported in  $\text{UTe}_2$ . In addition, there are indications for spontaneously broken time-reversal symmetry [186], and chiral Majorana edge and surface states [187], the na-

ture of which are not yet understood. Brun, Cren, and Roditchev summarized the superconductivity of 2D materials as a strong case for epitaxial monolayer materials growth [188].

#### D. Topological Properties

The study of conducting states in topologically non-trivial materials is often hindered by the presence of bulk conducting states [189]. High quality thin films offer one way of minimizing bulk contributions by increasing a sample's surface area-to-volume ratio, simplifying measurements of these topological effects. Due the nature of their electronic structure, actinide materials represent a fascinating, albeit challenging area for topological discoveries. Promising technological applications and insights into fundamental physics continue to motivate investigations on the complex manifold of  $5f$ ,  $6p$ ,  $6d$ , and  $7s$  orbital shells [190]. These interactions, present in an analogous manner in the rare earths, are expected to give rise to a variety of topological behaviors in different compounds and geometries.

Heavy fermion materials owe their particular properties to the competition between Coulomb repulsion of localized  $f$  electrons, and hybridization with itinerant  $d$  electrons. These electron correlations produce complex states including Mott physics, superconductivity, and correlated magnetism [191]. Understanding these electronic systems could potentially help elucidate other strongly correlated electron materials, for example high-temperature superconductors, multiferroics, and magnetoresistive materials. Topological insulators possess conducting surface states protected by the non-trivial topological property of spin-momentum locking. Several quantum materials have been proposed based on topological properties that involve quantum phenomena such as Majorana fermions, the anomalous quantum Hall effect, with applications in spintronics and fault tolerant quantum computation. Magnetic topological semimetals have been synthesized using MBE [192, 193]. These materials have a FM ground state that breaks time-reversal symmetry with a gap in the topological surface states [194]. A powerful tool to study these phenomena is density functional theory (DFT), e.g. its use in identifying phases in UNiSn corresponding to a topological insulator and a Weyl semimetal depending on magnetic ordering [195]. Rocksalt compounds of Pu and Am were predicted to form a topologically insulating ground state due to their  $5f$  electron being right on the boundary between localized and itinerant, and coupling between electronic and spin-orbit interactions gives rise to band gap formation [196]. The predicted compounds that Zhang *et al.* used for this study include americium monpnictides and plutonium monochalcogenide [196]. Using nuclear magnetic resonance (NMR), Dioguadi *et al.* demonstrated that PuB<sub>4</sub> is a strong candidate for a topological insulator, which has also been suggested by

Choi *et al.* [197, 198]. Recent theoretical work suggests that the intermediate valence PuB<sub>6</sub> is a strong topological insulator with nontrivial  $\mathbf{Z}_2$  topological invariants [199], similar to SmB<sub>6</sub> [200].

Overall, much work is still to be done in understanding fully the properties of these actinide compounds, and high quality thin films promise to be the missing piece to provide a window into their discovery.

#### V. CHALLENGES WITH MODELLING 5F ELECTRONS

DFT [201, 202] is normally the zeroth level of first-principles theory that is applied to any material, given the relatively small computational cost for the degree of complexity it can capture [203, 204]. DFT has found success across the periodic table for calculating a myriad of materials properties [205–208]. Unfortunately, all known implementations of DFT have well-known limitations [209–211]. In particular, DFT sometimes *qualitatively* breaks down for certain properties in materials bearing strongly correlated electrons. For example, Mott insulators are often incorrectly predicted to be metals by DFT. [212] Materials with  $f$ -electrons are ripe for strongly correlated electron physics, due to the relatively narrow bands formed by the  $f$ -orbitals and large on-site Coulomb repulsion. Other limitations for DFT calculations, particularly in strongly correlated systems, include the inability to properly capture finite temperatures and excited states [213].

Fortunately, dynamical mean-field theory (DMFT) [214] can overcome many of the shortcomings of DFT. DMFT can also be applied to real materials when combined with DFT to yield the DFT+DMFT formalism [210]. DMFT requires the solution of a quantum impurity problem, which is associated with the correlated shell of electrons (e.g.  $f$ -electrons). These solutions can be achieved in realistic multiorbital problems using continuous time quantum Monte-Carlo (CTQMC) [215–217]. While DFT+DMFT(CTQMC) is far more computationally expensive than DFT, current algorithms and computing power allow for calculations in relatively complex systems bearing  $d$  and  $f$  electrons [218–223]. An efficient, but far less accurate solution of the DMFT impurity problem can be achieved with the Hartree-Fock method. This method yields the better known DFT+ $U$  approach [210, 224], for which the computational overhead is negligible when compared to DFT. Together, DFT, DFT+DMFT, and DFT+ $U$  form a hierarchy of first-principles approaches that serve as the basis for parameterizing multiscale models to generate information at longer length and time scales [225].

Compared with bulk materials, the surfaces and heterostructures associated with thin films introduce additional complexity to modeling efforts due to confinement effects, charge transfer, strain, and structural reconstruc-

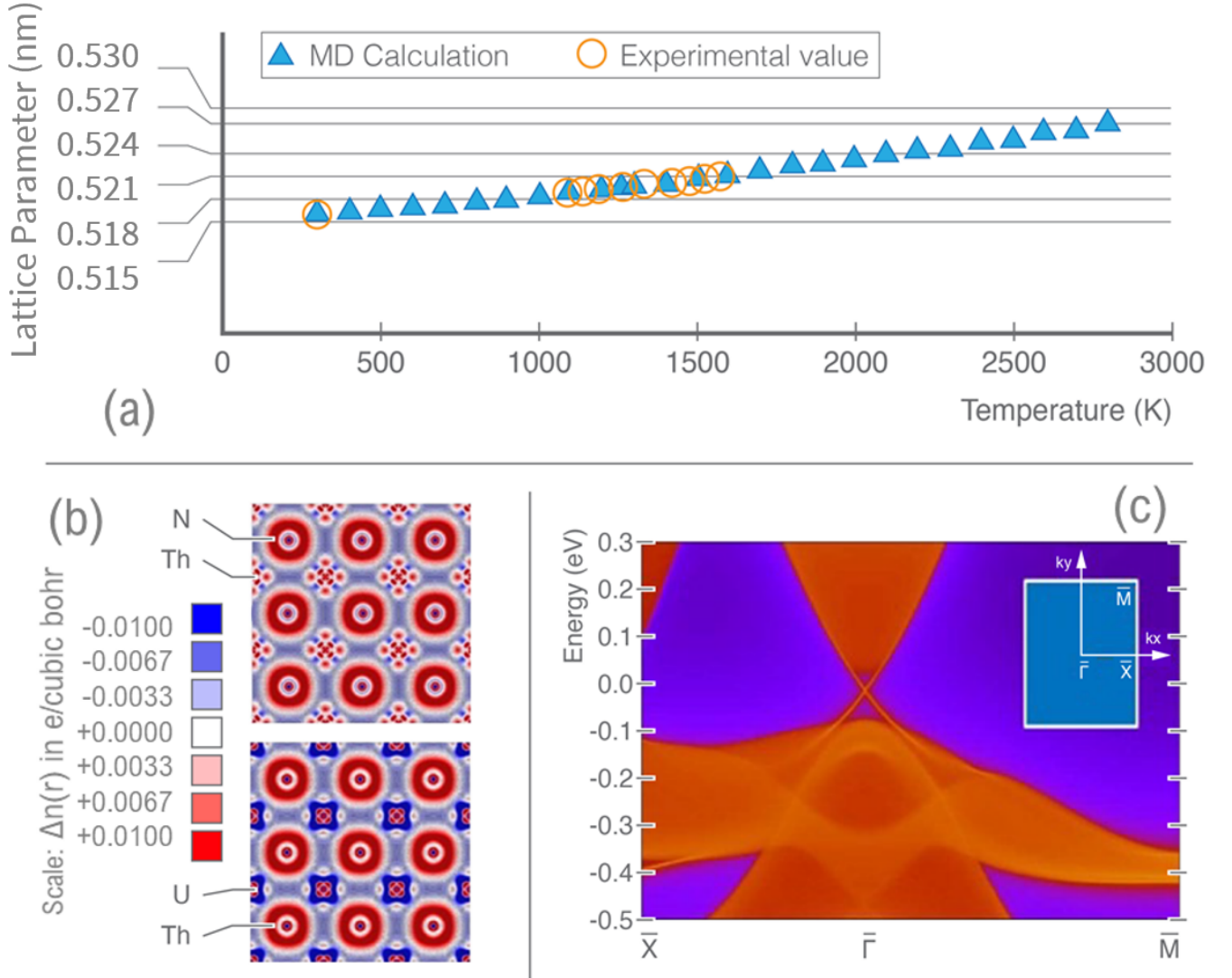


FIG. 4. (a) Comparison between the experimental thorium nitride lattice parameter as a function of temperature, and values calculated using molecular dynamics (MD) simulations [226]. Reproduced with permission from Elsevier. (b) Electron density plots calculated on the (001) plane for UN and ThN [227]. Reproduced with permission from the American Physical Society. (c) Band structure and energy spectrum of AmN, showing spin-orbit coupling interactions and a Dirac surface cone. From [196]. Reproduced with permission of AAAS.

tion. When considering actinide thin films, the presence of  $f$ -electrons in these systems contributes yet another layer of complexity. In actinide oxides, a wide range of phenomena have been observed in thin film heterostructures that are absent from their bulk constituents. These phenomena include superconductivity [228, 229], room temperature ferromagnetism [230], metal-insulator transitions [231], and orbital reconstruction [232], with the clear potential for novel device physics [233]. DFT+ $U$  and DFT+DMFT have already been used to confirm emergent properties in heterostructures composed from transition metal oxides [234–236]. However, similar calculations for heterostructures built from  $f$ -electron materials will undoubtedly be more challenging than those

for  $d$ -electron materials. The DFT+DMFT computations will be substantially more computationally expensive, and DFT+ $U$  computations will struggle with a more treacherous energy landscape. Nonetheless,  $f$ -electron heterostructures are within reach of our present theories and computational resources, and there has already been some progress at the level of DFT. Gao and Asok used DFT to study the (001), [237] and (111) [238] surfaces of Am. The surface properties of UN, a candidate nuclear fuel, have been studied using DFT+ $U$ , with potential applications for understanding corrosion characteristics [239]. In short, a combination of models based on DFT, DFT+ $U$ , and DFT+DMFT are well poised to study heterostructures composed from  $f$ -electron mate-

rial thin films, and will lay the foundation for understanding such materials.

Optimization of algorithms based on strongly correlated electron systems in DFT will provide more accurate descriptions of physical systems, able to in turn provide higher level modelling systems a path towards integration with engineering-level modelling paradigms based on first principles.

## VI. FUTURE DIRECTIONS: THIN FILM HETEROSTRUCTURE SYNTHESIS AND CHALLENGES

Interfaces in semiconducting, metallic, and semi-metallic materials offer possibilities for investigating electronic properties not typically present in the bulk, or in layers of a single material. In non-actinide semiconductors, heterostructures built by stacking different thin films have enabled researchers to discover new physics. For example, thin films and other low dimensional heterostructures allow to study the quantum behavior of charge carriers whose de Broglie wavelength is equivalent to the size of the potential well within which they are confined. A deeper understanding of how we can manipulate charge carrier behavior using heterostructures led to the design of entirely new electronic and photonic devices. Indeed, Kroemer famously stated that in these heterostructures, the interface *is* the device [240]. Extending heterostructure growth to actinide-based compounds therefore promises to enable researchers to study these materials in new ways. For example, low-dimensional heterostructures composed of actinide materials with  $5f$  electrons, grown with interfaces containing tailored defect densities, represent a fertile area for the discovery of various emerging phenomena [241]. Studies have predicted a range of exotic physics for such structures, including highly correlated electron interactions [190, 242], topological insulator behavior [195, 198], and confined 2D properties [243, 244].

As we have seen, the synthesis of high quality, atomically precise thin films of a *single* actinide material is still the focus of ongoing research. As a consequence, the ability to routinely and controllably integrate two or more of these thin films to create actinide heterostructures remains largely an area for future development. Before one can begin to study the characteristics of these heterostructures, one must first be able to produce high purity films with uncontaminated interfaces. Controlling interactions at the interface between two films requires a consideration of atomic intermixing, surface energies, charge transfer, and epitaxial nucleation and growth. These effects will likely be a function of the environment within which a heterostructure is synthesized [245]. Solution- and chemical reaction-based synthesis approaches, for example, often leave residues of unwanted atomic species during deposition. For this reason, physical deposition methods offer perhaps the best

route to achieving pristine thin film formation, and hence heterostructure synthesis. Due to its rapid output and relatively low cost, pulsed laser deposition offers a convenient test-bed for initial film and substrate screening studies. After some of the film-substrate combinations predicted by theory have been demonstrated experimentally, even higher quality films can be grown using molecular beam epitaxy (MBE), which uses ultrahigh purity elemental source materials rather than chemical precursors or solutions. The advantages of MBE include exceptionally high material purity, and exquisite control over layer thickness and interfacial abruptness, both of which are prerequisites for growing functional heterostructures. To our knowledge, MBE has not yet been used for the synthesis of actinide thin films or heterostructures.

The epitaxial challenges for integrating different materials include lattice constant mismatch, dissimilar crystal structures, thermal expansion differences, and incompatible growth environments. Several strategies have been devised to overcome strain-related issues arising from lattice mismatch. These include the use of graded buffers [246, 247], interfacial misfit arrays [248], self-assembled quantum dots [249], alloying [250], lattice constant mismatch inversion [251], and strain-relieving superlattices [252]. To accommodate different crystal structures, a common crystal lattice parameter can be used to geometrically align the lattices between each layer. An example is the differing crystal structures of ErAs (rock-salt) and InGaAs (zincblende). A rotation of the ErAs unit cell with respect to that of the InGaAs brings the two lattices into registry, enabling the growth of coherent ErAs/InGaAs heterostructures [253]. Mismatch between thermal expansion coefficients in different layers of the heterostructure can induce strain upon sample cooling, which is then relaxed through defect formation, negatively impacting crystal quality. Common solutions to this challenge include growth of thin protective thermal layers that prevent these relaxation processes, and use of thermally pre-stressed films that can accommodate the strain upon the change in temperature [254]. It will be critical to consider all of these challenges and solutions as researchers begin to explore the synthesis of actinide-based thin film heterostructures.

To fill this technological gap, the Idaho National Lab has recently commissioned an MBE system designed specifically for the growth of actinide-nitride compounds. This first-of-its-kind MBE system will permit feasibility studies of the growth of various actinide-based thin films. Proof-of-concept experiments will target the MBE growth of heterostructures based on UN and ThN (Figure 5). These heterostructures will enable the study of the electronic properties of these interesting  $5f$ -electron heterointerfaces. Given the lattice mismatch of  $\sim 5.7\%$  between UN and ThN, the substrate material must be chosen carefully to allow growth of layers with reasonable thickness, while remaining below the Matthews-Blakeslee limit for strain relaxation [255].

An alternative approach is to create heterostructures



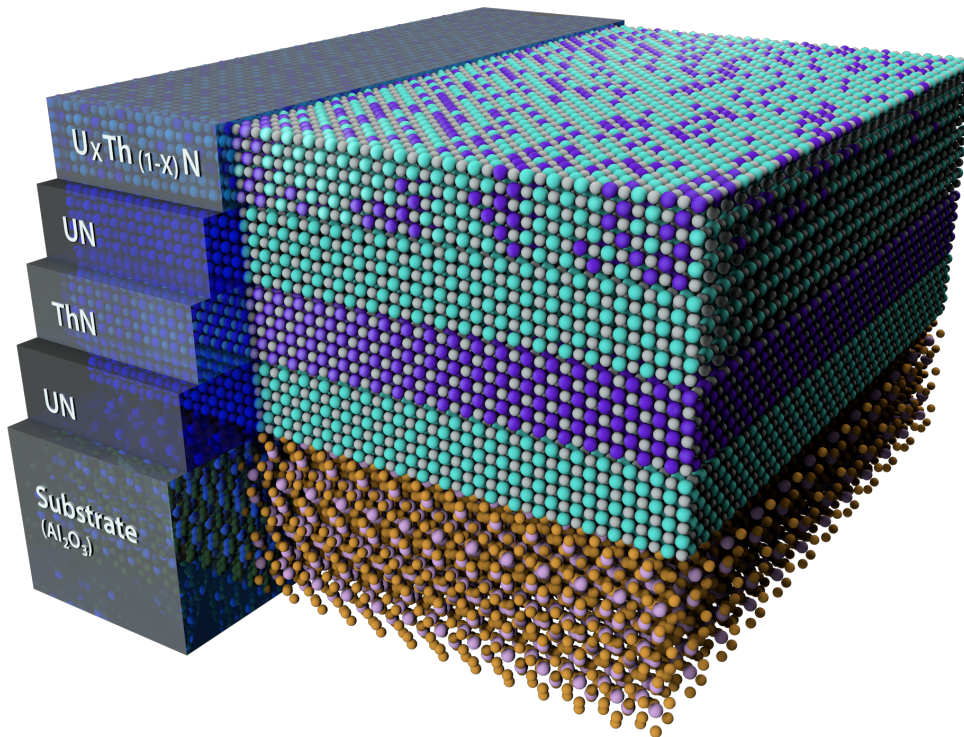


FIG. 5. Sketch of a proposed heterostructure consisting of alternating UN and ThN thin films. In practice, to avoid strain relaxation, the maximum allowed thickness of each layer must be calculated from the Matthews-Blakeslee equation [255].

based on  $U_xTh_{1-x}N$  alloys that have lower lattice mismatch to the binary end-point compounds. To this end, Table IV lists a “recipe book” of actinide nitrides and candidate substrates with reasonably lattice-matched alloys. Indeed, by incorporating suitable buffer layers, some of these compound/substrate combinations have already been synthesized [45]. The hope is that by exploring the MBE growth of materials in these actinide nitride systems, their thermophysical, magnetic, and topological properties can be studied with high precision. Actinide-nitride-based systems that show promising initial results will be screened for emergent phenomena, with a view to opening a new approach to investigating the interplay between electronic correlations and topology in epitaxial thin films and heterostructures.

## VII. OUTLOOK

Recent years have seen significant advances in the field of actinide materials synthesis. Ongoing improvements in materials growth techniques are beginning to produce single-crystal samples of actinide metals and their compounds. These efforts include the synthesis of both bulk crystals and thin films, within which grain boundaries are eliminated and the density of other crystallographic defects is reduced. Syntheses using a variety of methods have been demonstrated important initial material

compatibility criteria (temperature ranges, lattice constants, etc.) for reliable thin film synthesis. As a result, researchers can, for the first time, investigate thermal and electrical transport properties of actinides in samples with dramatically reduced phonon and electron scattering. In the near term, concerted efforts are being made to integrate different thin film actinides into heterostructures whose properties can be tuned through strain, confinement and other interfacial effects. The expectation is that, as a result, the subtle physical features of these materials will begin to emerge. Exotic magnetic and topological properties are expected to arise in these strongly correlated systems with  $5f$ -shell electrons, leading to the discovery of new physics.

## ACKNOWLEDGEMENTS

This work was supported through the INL Laboratory Directed Research & Development Program under U.S. Department of Energy Idaho Operations Office Contract DE-AC07-05ID14517. F.K. acknowledges the support of the Glenn T. Seaborg Institute for Actinide Science at Idaho National Laboratory. C.A.M and D.H.H. acknowledge support from the Center for Thermal Energy Transport under Irradiation (TETI), an Energy Frontier Research Center funded by the US Department of Energy, Office of Science, Office of Basic Energy Sciences. The

TABLE IV. Crystallographic properties of UN and ThN thin films and candidate substrates.

Material	Group	$a$ (Å)	$c$ (Å)	Substrate	Substrate lattice const. (Å)	Strain
UN	Fm $\bar{3}$ m	4.88	4.88	$\langle 001 \rangle_{\text{UN}} \parallel \langle 001 \rangle_{\text{Al}_2\text{O}_3}$	4.785	1.96%
	Fm $\bar{3}$ m	4.88	4.88	$\langle 001 \rangle_{\text{UN}} \parallel \langle 111 \rangle_{\text{Si}}$	3.135	<i>relaxed</i>
	Fm $\bar{3}$ m	4.88	4.88	$\langle 001 \rangle_{\text{UN}} \parallel \langle 111 \rangle_{\text{NaF}}$	4.62	5.84%
UN <sub>2</sub>	Fm $\bar{3}$ m	5.31	5.31	$\langle 111 \rangle_{\text{UN}_2} \parallel \langle 001 \rangle_{\text{LAO}}$	3.79	[256]
	Fm $\bar{3}$ m	5.31	5.31	$\langle 100 \rangle_{\text{UN}_2} \parallel \langle 001 \rangle_{\text{ZnS}}$	5.41	1.02%
	Fm $\bar{3}$ m	5.31	5.31	$\langle 100 \rangle_{\text{UN}_2} \parallel \langle 001 \rangle_{\text{GaAs}}$	5.3565	0.7%
	Fm $\bar{3}$ m	5.31	5.31	$\langle 100 \rangle_{\text{UN}_2} \parallel \langle 001 \rangle_{\text{Si}}$	5.43	2.26%
$\alpha$ -U <sub>2</sub> N <sub>3</sub>	Ia $\bar{3}$	10.684	10.684	$\langle 001 \rangle_{\text{U}_2\text{N}_3} \parallel \langle 001 \rangle_{\text{Y}_2\text{O}_3}$	10.64	0.75%
$\beta$ -U <sub>2</sub> N <sub>3</sub>	Ia $\bar{3}$	3.69	5.826	$\langle 001 \rangle_{\text{U}_2\text{N}_3} \parallel \langle 001 \rangle_{\text{CaF}_2}$	5.47	2.05% (2:1 relation)
ThN	Fm $\bar{3}$ m	5.20	5.20	$\langle 001 \rangle_{\text{ThN}} \parallel \langle 001 \rangle_{\text{CaF}_2}$	5.47	5.37%
	Fm $\bar{3}$ m	5.20	5.20	$\langle 001 \rangle_{\text{ThN}} \parallel \langle 001 \rangle_{\text{YSZ}}$	5.125	0.76%
	Fm $\bar{3}$ m	5.20	5.20	$\langle 001 \rangle_{\text{ThN}} \parallel \langle 001 \rangle_{\text{Si}}$	5.43	5.00%
Th <sub>2</sub> N <sub>3</sub>	C $\bar{3}$ m	3.875	6.175	$\langle 001 \rangle_{\text{Th}_2\text{N}_3} \parallel \langle 001 \rangle_{\text{LAO}}$	3.79	2.19%
Th <sub>3</sub> N <sub>4</sub>	R $\bar{3}$ m	3.875	27.39	$\langle 001 \rangle_{\text{Th}_3\text{N}_4} \parallel \langle 001 \rangle_{\text{LAO}}$	3.79	2.19%

authors would like to thank A. Tiwari at the University of Utah for useful discussions. K.D.V. acknowledges the support of his herds of guinea pigs and hamster.

## REFERENCES

- [1] L R Morss, N M Edelstein, J Fuger, and J J Katz. *The chemistry of the actinide and transactinide elements*, volume 1. Springer, 2006.
- [2] K Mattenberger, O Vogt, J C Spirlet, and J Rebizant. Anisotropic magnetization of PuAs, PuSb and PuBi single crystals. *Journal of magnetism and magnetic materials*, 54:539–540, 1986.
- [3] E Enriquez, G Wang, Y Sharma, I Sarpkaya, Q Wang, D Chen, N Winner, X Guo, J Dunwoody, J White, and *et al.* Structural and optical properties of phase-pure UO<sub>2</sub>,  $\alpha$ -U<sub>3</sub>O<sub>8</sub>, and  $\alpha$ -UO<sub>3</sub> epitaxial thin films grown by pulsed laser deposition. *ACS Applied Materials & Interfaces*, 12(31):35232–35241, 2020.
- [4] D H Hurley, A El-Azab, M S Bryan, M W D Cooper, C A Dennett, K Gofryk, L He, M Khafizov, G H Lander, M E Manley, and *et al.* Thermal energy transport in oxide nuclear fuel. *Chemical Reviews*, 122(3):3711–3762, 2022.
- [5] K Rickert, M A Velez, T A Prusnick, D B Turner, M M Kimani, T Bowen, and J M Mann. Hydrothermal crystal growth on non-native substrates: The case of UO<sub>2</sub>. *Crystal Growth & Design*, 21(11):6289–6300, 2021.
- [6] T Gouder. Thin layers in actinide research. *Journal of alloys and compounds*, 271:841–845, 1998.
- [7] K Mudiyansele, A K Burrell, S D Senanayake, and H Idriss. XPS and NEXAFS study of the reactions of acetic acid and acetaldehyde over UO<sub>2</sub>(100) thin film. *Surface Science*, 680:107–112, feb 2019.
- [8] J C Spirlet and O Vogt. Preparation of actinides and actinide compounds. *Journal of Magnetism and Magnetic Materials*, 29(1-3):31–38, 1982.
- [9] C R Edwards and A J Oliver. Uranium processing: a review of current methods and technology. *Jom*, 52(9):12–20, 2000.
- [10] K M Glover and P Borrell. A method for the preparation of thin films of plutonium and uranium. *Journal of Nuclear Energy*, 1(3-4):214–217, 1955.
- [11] T Durakiewicz, J J Joyce, G H Lander, C G Olson, M T Butterfield, E Guziewicz, A J Arko, L Morales, J Rebizant, K Mattenberger, and *et al.* Electronic structure of actinide antimonides and tellurides from photoelectron spectroscopy. *Physical Review B*, 70(20):205103, 2004.
- [12] J D Farr, A L Giorgi, M C Bowman, and R K Money. The crystal structure of actinium metal and actinium hydride. Technical report, Los Alamos National Laboratory (LANL), Los Alamos, NM (United States), 1953.
- [13] A L Bowman and G P Arnold. The crystal structure of Th<sub>3</sub>N<sub>4</sub>. *Acta Crystallographica Section B: Structural Crystallography and Crystal Chemistry*, 27(1):243–244, 1971.
- [14] H Tagawa and N Masaki. X-ray and density studies of nonstoichiometric uranium sesquinitride. *Journal of Inorganic and Nuclear Chemistry*, 36(5):1099–1103, 1974.
- [15] V M Radchenko, M A Ryabinin, and V A Stupin. Production and investigation of thin films of metal actinides (Pu, Am, Cm, Bk, Cf). *IOP Conference Series: Materials Science and Engineering*, 9(1):012034, 2010.
- [16] I D Danilin, V D Kartushin, N V Pilipenko, I D Abramycheva, and S P Vesnovskii. Production of films of uranium and americium compounds by thermal decomposition of volatile  $\beta$ -diketonates. *Nuclear Instruments and Methods in Physics Research Section A: Accelerators, Spectrometers, Detectors and Associated Equipment*, 480(1):75–78, 2002.
- [17] I Kruk, B L Scott, E B Watkins, and L E Wolfsberg. Growth and characterization of uranium oxide thin films deposited by polymer assisted deposition. *Thin Solid Films*, 735:138874, 2021.
- [18] A K Burrell, T M McCleskey, P Shukla, H Wang, T Durakiewicz, D P Moore, C G Olson, J J Joyce, and Q Jia. Controlling oxidation states in uranium oxides through epitaxial stabilization. *Advanced materials*, 19(21):3559–3563, 2007.

- [19] B L Scott, J J Joyce, T D Durakiewicz, R L Martin, T M McCleskey, E Bauer, H Luo, and Q Jia. High quality epitaxial thin films of actinide oxides, carbides, and nitrides: Advancing understanding of electronic structure of *f*-element materials. *Coordination Chemistry Reviews*, 266:137–154, 2014.
- [20] M T McCleskey, E Bauer, Q Jia, A K Burrell, B L Scott, S D Conradson, A Mueller, L Roy, X Wen, G E Scuseria, and *et al.* Optical band gap of  $\text{NpO}_2$  and  $\text{PuO}_2$  from optical absorbance of epitaxial films. *Journal of Applied Physics*, 113(1):013515, 2013.
- [21] N Getoff and H Bildstein. Molecular plating: VI. quantitative electrodeposition of americium. *Nuclear Instruments and Methods*, 70(3):352–354, 1969.
- [22] R A A Muzzarelli. The preparation of thin films of tantalum and protactinium by electro spraying. *Inorganic and Nuclear Chemistry Letters*, 2(1):1–3, 1966.
- [23] H Shimojima and J Takagi. Electrodeposition of protactinium. *Journal of Inorganic and Nuclear Chemistry*, 26(2):253–255, 1964.
- [24] S R Qiu, C Amrhein, M L Hunt, R Pfeffer, B Yakshinskiy, L Zhang, T E Madey, and J A Yarmoff. Characterization of uranium oxide thin films grown from solution onto Fe surfaces. *Applied surface science*, 181(3-4):211–224, 2001.
- [25] R A Laudise. Hydrothermal synthesis of crystals. *50 years Progress in Crystal Growth*, page 185, 2004.
- [26] C Young, J Petrosky, J M Mann, E M Hunt, D Turner, and T Kelly. The work function of hydrothermally synthesized  $\text{UO}_2$  and the implications for semiconductor device fabrication. *physica status solidi (RRL)–Rapid Research Letters*, 10(9):687–690, 2016.
- [27] C L Dugan, G G Peterson, A Mock, C Young, J M Mann, M Nastasi, M Schubert, L Wang, W Mei, I Tanabe, and *et al.* Electrical and material properties of hydrothermally grown single crystal (111)  $\text{UO}_2$ . *The European Physical Journal B*, 91(4):1–7, 2018.
- [28] Y Huentupil, G Cabello-Guzmán, B Chornik, R Arancibia, and G E Buono-Core. Photochemical deposition, characterization and optical properties of thin films of  $\text{ThO}_2$ . *Polyhedron*, 157:225–231, 2019.
- [29] K Rickert, T A Prusnick, E Hunt, A French, D B Turner, C A Dennett, L Shao, and J M Mann. Raman and photoluminescence evaluation of ion-induced damage uniformity in  $\text{ThO}_2$ . *Nuclear Instruments and Methods in Physics Research Section B: Beam Interactions with Materials and Atoms*, 515:69–79, 2022.
- [30] A Majumdar, K V Manukyan, S Dede, J M Roach, D Robertson, P C Burns, and A Aprahamian. Irradiation-driven restructuring of  $\text{UO}_2$  thin films: Amorphization and crystallization. *ACS Applied Materials & Interfaces*, 13(29):35153–35164, 2021.
- [31] M D Straub, J Leduc, M Frank, A Raauf, T D Lohrey, S G Minasian, S Mathur, and J Arnold. Chemical vapor deposition of phase-pure uranium dioxide thin films from uranium (IV) amidate precursors. *Angewandte Chemie International Edition*, 58(17):5749–5753, 2019.
- [32] A Raauf, J Leduc, M Frank, D Stadler, D Graf, M Wilhelm, M Grosch, and S Mathur. Magnetic field-assisted chemical vapor deposition of  $\text{UO}_2$  thin films. *Inorganic Chemistry*, 60(3):1915–1921, 2021.
- [33] L Tarnawska, A Giussani, P Zaumseil, M A Schubert, R Paszkiewicz, O Brandt, P Storck, and T Schroeder. Single crystalline  $\text{Sc}_2\text{O}_3/\text{Y}_2\text{O}_3$  heterostructures as novel engineered buffer approach for GaN integration on Si (111). *Journal of Applied Physics*, 108(6):063502, 2010.
- [34] L-Å Ragnarsson, S Guha, M Copel, E Cartier, N A Bojarczuk, and J Karasinski. Molecular-beam-deposited yttrium-oxide dielectrics in aluminum-gated metal-oxide-semiconductor field-effect transistors: Effective electron mobility. *Applied Physics Letters*, 78(26):4169–4171, 2001.
- [35] T Mori. Thermoelectric and magnetic properties of rare earth borides: Boron cluster and layered compounds. *Journal of Solid State Chemistry*, 275:70–82, 2019.
- [36] I Ohkubo, T Aizawa, K Nakamura, and T Mori. Control of competing thermodynamics and kinetics in vapor phase thin-film growth of nitrides and borides. *Frontiers in Chemistry*, 9:528, 2021.
- [37] Z Li, J Kim, N Kioussis, S Ning, H Su, T Iitaka, T Tohyama, X Yang, and J Zhang. GdN thin film: Chern insulating state on square lattice. *Physical Review B*, 92(20):201303, 2015.
- [38] K H Goh, A S M A Haseeb, and Y H Wong. Lanthanide rare earth oxide thin film as an alternative gate oxide. *Materials Science in Semiconductor Processing*, 68:302–315, 2017.
- [39] M Leskelä, K Kukli, and M Ritala. Rare-earth oxide thin films for gate dielectrics in microelectronics. *Journal of Alloys and Compounds*, 418(1-2):27–34, 2006.
- [40] J E Johnson, D D Allred, R S Turley, W R Evans, and R L Sandberg. Thorium-based thin films as highly reflective mirrors in the EUV. *MRS Online Proceedings Library (OPL)*, 893, 2005.
- [41] N F Brimhall, A B Grigg, R S Turley, and D D Allred. Thorium dioxide thin films in the extreme ultraviolet. In *Advances in X-Ray/EUV Optics, Components, and Applications*, volume 6317, page 631710. International Society for Optics and Photonics, 2006.
- [42] M Bagge-Hansen, R A Outlaw, K Seo, and D M Manos. Morphology and crystallization of  $\text{ThO}_2$  thin films on polycrystalline Ir. *Thin solid films*, 520(13):4249–4253, 2012.
- [43] M Uno, M Katsura, and M Miyake. Preparation of  $\text{Th}_3\text{N}_4$  and its oxidation behaviour. *Journal of the Less Common Metals*, 135(1):25–38, 1987.
- [44] T Gouder, L Havela, L Black, F Wastin, J Rebizant, P Boulet, D Bouexiere, S Heathman, and M Idiri. Synthesis and electronic properties of Th–N films. *Journal of alloys and compounds*, 336(1-2):73–76, 2002.
- [45] E L Bright, S Rennie, M Cattelan, N A Fox, D T Goddard, and R Springell. Epitaxial UN and  $\alpha\text{-U}_2\text{N}_3$  thin films. *Thin Solid Films*, 661:71–77, 2018.
- [46] L Black, F Miserque, T Gouder, L Havela, J Rebizant, and F Wastin. Preparation and photoelectron spectroscopy study of  $\text{UN}_x$  thin films. *Journal of alloys and compounds*, 315(1-2):36–41, 2001.
- [47] Z Long, Y Hu, L Chen, L Luo, K Liu, and X Lai.  $\text{Un}_{2-x}$  layer formed on uranium metal by glow plasma nitriding. *Journal of Alloys and Compounds*, 620:289–293, 2015.
- [48] T Gouder. Electronic structure of uranium overlayers on magnesium and aluminium. *Surface science*, 382(1-3):26–34, 1997.
- [49] A. M. Adamska, Springell Scott, T. B., R., A. D. Waren, L. Pico, and O. Payton. Growth and characterization of uranium-alloy thin films, Apr 2014.



- [50] M Eckle and T Gouder. Photoemission study of  $\text{UN}_x\text{O}_y$  and  $\text{UC}_x\text{O}_y$  in thin films. *Journal of alloys and compounds*, 374(1-2):261–264, 2004.
- [51] T K Bierlein and B Mastel. Damage in  $\text{UO}_2$  films and particles during reactor irradiation. *Journal of Applied Physics*, 31(12):2314–2315, 1960.
- [52] M S Elbakhshwan and B J Heuser. Structural and compositional characterization of single crystal uranium dioxide thin films deposited on different substrates. *Thin Solid Films*, 636:658–663, 2017.
- [53] Y A Teterin, A J Popel, K I Maslakov, A Y Teterin, K E Ivanov, S N Kalmykov, R Springell, T B Scott, and I Farnan. XPS study of ion irradiated and unirradiated  $\text{UO}_2$  thin films. *Inorganic chemistry*, 55(16):8059–8070, 2016.
- [54] A J Popel, A M Adamska, P G Martin, O D Payton, G I Lampronti, L Picco, L Payne, R Springell, T B Scott, I Monnet, C Grygiel, and I Farnan. Structural effects in  $\text{UO}_2$  thin films irradiated with U ions. *Nuclear Instruments and Methods in Physics Research Section B: Beam Interactions with Materials and Atoms*, 386:8–15, 2016.
- [55] S Rennie, E L Bright, J E Darnbrough, L Paolasini, A Bosak, A D Smith, N Mason, G H Lander, and R Springell. Study of phonons in irradiated epitaxial thin films of  $\text{UO}_2$ . *Physical Review B*, 97(22):224303, 2018.
- [56] K I Maslakov, Y A Teterin, A J Popel, A Y Teterin, K E Ivanov, S N Kalmykov, V G Petrov, R Springell, T B Scott, and I Farnan. XPS study of the surface chemistry of  $\text{UO}_2$  (111) single crystal film. *Applied Surface Science*, 433:582–588, 2018.
- [57] D Zhang, H Dong, Y Lou, Y Zhong, F Li, X Fu, Y Zheng, and W Li. Optical properties, band structures, and phase transition of  $\text{UO}_{2+x}$  epitaxial films deposited by polymer-assisted deposition. *AIP Advances*, 11(11):115107, 2021.
- [58] J M Roach, K V Manukyan, A Majumdar, S Dede, A G Oliver, P C Burns, and A Aprahamian. Hyperstoichiometric uranium dioxides: Rapid synthesis and irradiation-induced structural changes. *Inorganic Chemistry*, 60(24):18938–18949, 2021.
- [59] P Cakir, R Eloirdi, F Huber, R J M Konings, and T Gouder. Surface reduction of neptunium dioxide and uranium mixed oxides with plutonium and thorium by photocatalytic reaction with ice. *The Journal of Physical Chemistry C*, 119(3):1330–1337, 2015.
- [60] N R Miljević and Z S Žunić. Environmental and health impact assessment of ammunition containing transuranic elements. In *Environmental Consequences of War and Aftermath*, pages 209–251. Springer, 2009.
- [61] J Shaw, A Whittaker, L Polley, and G Wortley. Preparation of thin uniform films of  $\text{PuO}_2$  suitable for fission fragment counting. Technical report, United Kingdom Atomic Energy Authority, Sellafield, Cumb., England (United Kingdom), 1958.
- [62] M P Wilkerson, J M Dorhout, K S Graham, J J Joyce, I I Kruk, J Majewski, D T Olive, A L Pugmire, B L Scott, J T Stritzinger, and *et al.* Structural properties, thicknesses, and qualities of plutonium oxide thin films prepared by polymer assisted deposition. *Surface Science*, 701:121696, 2020.
- [63] P Roussel. Inverse photoemission measurements of plutonium metal and oxides. *Journal of Electron Spectroscopy and Related Phenomena*, 246:147030, 2021.
- [64] C B Finch and G W Clark. High-temperature solution growth of single-crystal neptunium dioxide. *Journal of Crystal Growth*, 6(3):245–248, 1970.
- [65] C B Finch and G W Clark. High-temperature solution growth of single-crystal plutonium dioxide. *Journal of Crystal Growth*, 12(2):181–182, 1972.
- [66] A Modin, Y Yun, M-T Suzuki, J Vegelius, L Werme, J Nordgren, P M Oppeneer, and S M Butorin. Indication of single-crystal  $\text{PuO}_2$  oxidation from O 1s x-ray absorption spectra. *Physical Review B*, 83(7):075113, 2011.
- [67] D Mannix, S Langridge, G H Lander, J Rebizant, M J Longfield, W G Stirling, W J Nuttall, S Coburn, S Wasserman, and L Soderholm. Experiments on transuranium compounds with x-ray resonant exchange scattering. *Physica B: Condensed Matter*, 262(1-2):125–140, 1999.
- [68] T Gouder, F Wastin, J Rebizant, and L Havela. 5f electron localization in  $\text{PuSe}$  and  $\text{PuSb}$ . *Physical review letters*, 84(15):3378, 2000.
- [69] D Rafaja, L Havela, R Kužel, F Wastin, E Colineau, and T Gouder. Real structure and magnetic properties of UN thin films. *Journal of alloys and compounds*, 386(1-2):87–95, 2005.
- [70] N-T H Kim-Ngan, A G Balogh, L Havela, and T Gouder. Ion beam mixing in uranium nitride thin films studied by rutherford backscattering spectroscopy. *Nuclear Instruments and Methods in Physics Research Section B: Beam Interactions with Materials and Atoms*, 268(11-12):1875–1879, 2010.
- [71] X Wang, Z Long, R Bin, R Yang, Q Pan, F Li, L Luo, Y Hu, and K Liu. Study of the decomposition and phase transition of uranium nitride under UHV conditions via TDS, XRD, SEM, and XPS. *Inorganic chemistry*, 55(21):10835–10838, 2016.
- [72] L Luo, Q Pan, Y Hu, K Liu, and X Wang. Insight into the initial oxidation of  $\text{UN}_{1.85}$  thin films. *Applied Surface Science*, 525:146535, 2020.
- [73] Z Long, L Luo, Y Lu, Y Hu, K Liu, and X Lai. Study on the electronic structure of  $\alpha\text{-U}_2\text{N}_3$  by XPS and first principles. *Journal of Alloys and Compounds*, 664:745–749, 2016.
- [74] Z Bao, R Springell, H C Walker, H Leiste, K Kuebel, R Prang, G Nisbet, S Langridge, RCC Ward, T Gouder, and *et al.* Antiferromagnetism in  $\text{UO}_2$  thin epitaxial films. *Physical Review B*, 88(13):134426, 2013.
- [75] A J Popel, V A Lebedev, P G Martin, A A Shiryaev, G I Lampronti, R Springell, S N Kalmykov, T B Scott, I Monnet, C Grygiel, and *et al.* Structural effects in  $\text{UO}_2$  thin films irradiated with fission-energy Xe ions. *Journal of Nuclear Materials*, 482:210–217, 2016.
- [76] Q Chen, X Lai, B Bai, and M Chu. Structural characterization and optical properties of  $\text{UO}_2$  thin films by magnetron sputtering. *Applied surface science*, 256(10):3047–3050, 2010.
- [77] S D Senanayake, G I N Waterhouse, H Idriss, and T E Madey. Coupling of carbon monoxide molecules over oxygen-defected  $\text{UO}_2$  (111) single crystal and thin film surfaces. *Langmuir*, 21(24):11141–11145, 2005.
- [78] T T Meek, B Von Roedern, P G Clem, and R J Hanrahan Jr. Some optical properties of intrinsic and doped

- uo2 thin films. *Materials Letters*, 59(8-9):1085–1088, 2005.
- [79] S Stumpf, A Seibert, T Gouder, F Huber, T Wiss, J Römer, and M A Denecke. Development of fuel-model interfaces: Characterization of Pd containing UO<sub>2</sub> thin films. *Journal of nuclear materials*, 397(1-3):19–26, 2010.
- [80] T Gouder, R Eloirdi, F Wastin, E Colineau, J Rebizant, D Kolberg, and F Huber. Electronic structure of UH<sub>3</sub> thin films prepared by sputter deposition. *Physical Review B*, 70(23):235108, 2004.
- [81] D Chaney, A Castellano, A Bosak, J Bouchet, F Bottin, B Dorado, L Paolasini, S Rennie, Christopher Bell, R Springell, et al. Tuneable correlated disorder in alloys. *Physical Review Materials*, 5(3):035004, 2021.
- [82] R C C Ward, R A Cowley, N Ling, W Goetze, G H Lander, and W G Stirling. The structure of epitaxial layers of uranium. *Journal of Physics: Condensed Matter*, 20(13):135003, 2008.
- [83] R Springell, R C C Ward, J Bouchet, J Chivall, D Wermeille, P S Normile, S Langridge, S W Zochowski, and G H Lander. Malleability of uranium: Manipulating the charge-density wave in epitaxial films. *Physical Review B*, 89(24):245101, 2014.
- [84] H Ladislav, M Paukov, M Dopita, L Horák, D Drozdenko, M Diviš, I Turek, D Legut, L Křývala, T Gouder, and et al. Crystal structure and magnetic properties of uranium hydride UH<sub>2</sub> stabilized as a thin film. *Inorganic chemistry*, 57(23):14727–14732, 2018.
- [85] R N R Mulford and T A Wiewandt. The neptunium-hydrogen system. *The Journal of Physical Chemistry*, 69(5):1641–1644, 1965.
- [86] L Havela, F Wastin, J Rebizant, and T Gouder. Photoelectron spectroscopy study of PuN. *Physical Review B*, 68(8):085101, 2003.
- [87] R N R Mulford and G E Sturdy. The plutonium-hydrogen system. I. plutonium dihydride and dideuteride. *Journal of the American Chemical Society*, 77(13):3449–3452, 1955.
- [88] J L Sarrao, L A Morales, J D Thompson, B L Scott, G R Stewart, F Wastin, J Rebizant, P Boulet, E Colineau, and G H Lander. Plutonium-based superconductivity with a transition temperature above 18 K. *Nature*, 420(6913):297–299, 2002.
- [89] Alice Seibert, T. Gouder, and F. Huber. Interaction of puo2 thin films with water. *Radiochimica Acta*, 98(9-11):647–657, 2010.
- [90] T Gouder, PM Oppeneer, F Huber, F Wastin, and J Rebizant. Photoemission study of the electronic structure of am, amn, amsb, and am 2 o 3 films. *Physical Review B*, 72(11):115122, 2005.
- [91] W M Olson and R N R Mulford. The americium—hydrogen system. *The Journal of Physical Chemistry*, 70(9):2934–2937, 1966.
- [92] B M Bansal and D Damien. Curium hydride. *Inorganic and Nuclear Chemistry Letters*, 6(7):603–606, 1970.
- [93] L Lu, F Li, H Xiao, Y Hu, L Luo, B Bai, J Liu, and K Liu. Thermal stability of uranium nitride and oxynitride films in an ultra-high vacuum environment. *Journal of Nuclear Materials*, 509:408–416, 2018.
- [94] A I Apostol, A Pantelica, I Ortega-Feliu, N Marginean, O Sima, M Straticiuc, M C Jimenez-Ramos, and V Fugaru. Ion beam analysis of elemental signatures in uranium dioxide samples: importance for nuclear forensics. *Journal of Radioanalytical and Nuclear Chemistry*, 311(2):1339–1346, 2017.
- [95] C A Dennett, Z Hua, A Khanolkar, T Yao, P K Morgan, T A Prusnick, N Poudel, A French, K Gofryk, L He, et al. The influence of lattice defects, recombination, and clustering on thermal transport in single crystal thorium dioxide. *APL Materials*, 8(11):111103, 2020.
- [96] S S Parker, S Newman, A J Fallgren, and J T White. Thermophysical properties of mixtures of thorium and uranium nitride. *Journal of Materials*, 73(11):3564–3575, 2021.
- [97] H F Jackson, D D Jayaseelan, W E Lee, M J Reece, F Inam, D Manara, C P Casoni, F De Bruycker, and K Boboridis. Laser melting of spark plasma-sintered zirconium carbide: thermophysical properties of a generation iv very high-temperature reactor material. *International Journal of Applied Ceramic Technology*, 7(3):316–326, 2010.
- [98] D P Daroca, S Jaroszewicz, A M Llois, and H O Mosca. Phonon spectrum, mechanical and thermophysical properties of thorium carbide. *Journal of nuclear materials*, 437(1-3):135–138, 2013.
- [99] T Gouder and L Havela. Examples of quantification in XPS on 5f materials. *Microchimica Acta*, 138(3):207–215, 2002.
- [100] J J Joyce, J M Wills, T Durakiewicz, M T Butterfield, E Guziewicz, D P Moore, J L Sarrao, L A Morales, A J Arko, O Eriksson, and et al. Dual nature of the 5f electrons in plutonium materials. *Physica B: Condensed Matter*, 378:920–924, 2006.
- [101] J J Joyce, T Durakiewicz, K S Graham, E D Bauer, D P Moore, J N Mitchell, J A Kennison, R L Martin, L E Roy, and G E Scuseria. Pu electronic structure and photoelectron spectroscopy. *Journal of Physics: Conference Series*, 273(1):012023, 2011.
- [102] R Eloirdi, L Havela, T Gouder, A Shick, J Rebizant, F Huber, and R Caciuffo. Photoelectron spectroscopy study of PuCoGa<sub>5</sub> thin films. *Journal of nuclear materials*, 385(1):8–10, 2009.
- [103] T Gouder, R Eloirdi, and R Caciuffo. Direct observation of pure pentavalent uranium in U<sub>2</sub>O<sub>5</sub> thin films by high resolution photoemission spectroscopy. *Scientific reports*, 8(1):1–7, 2018.
- [104] S Fujimori, T Ohkochi, T Okane, Y Saitoh, A Fujimori, H Yamagami, Y Haga, E Yamamoto, and Y Ōnuki. Itinerant nature of U 5f states in uranium mononitride revealed by angle-resolved photoelectron spectroscopy. *Phys. Rev. B*, 86(23):235108, 2012.
- [105] T Durakiewicz, P S Riseborough, C G Olson, J J Joyce, P M Oppeneer, S Elgazzar, E D Bauer, J L Sarrao, E Guziewicz, D P Moore, and et al. Observation of a kink in the dispersion of f-electrons. *Europhys. Lett.*, 84(3):37003, 2008.
- [106] T Das, T Durakiewicz, J-X Zhu, J J Joyce, J L Sarrao, and M J Graf. Imaging the formation of high-energy dispersion anomalies in the actinide UCoGa<sub>5</sub>. *Phys. Rev. X*, 2(4):041012, 2012.
- [107] I Kawasaki, S Fujimori, Y Takeda, T Okane, A Yasui, Y Saitoh, H Yamagami, Y Haga, E Yamamoto, and Y Ōnuki. Band structure and fermi surface of UPd<sub>3</sub> studied by soft x-ray angle-resolved photoemission spectroscopy. *Phys. Rev. B*, 87(7):075142, 2013.

- [108] M F Beaux II, T Durakiewicz, L Moreschini, M Grioni, F Offi, G Monaco, G Panaccione, J J Joyce, E D Bauer, J L Sarrao, and *et al.* Electronic structure of single crystal UPd<sub>3</sub>, UGe<sub>2</sub>, and USb<sub>2</sub> from hard X-ray and angle-resolved photoelectron spectroscopy. *Journal of Electron Spectroscopy and Related Phenomena*, 184(8-10):517–524, 2011.
- [109] J D Denlinger, G-H Gweon, J W Allen, C G Olson, M B Maple, J L Sarrao, P E Armstrong, Z Fisk, and H Yamagami. Comparative study of the electronic structure of URu<sub>2</sub>Si<sub>2</sub>: probing the anderson lattice. *Journal of Electron Spectroscopy and Related Phenomena*, 117:347–369, 2001.
- [110] T Ito, H Kumigashira, T Takahashi, Y Haga, E Yamamoto, T Honma, H Ohkuni, and Y. Ōnuki. Band structure and fermi surface of URu<sub>2</sub>Si<sub>2</sub> studied by high-resolution angle-resolved photoemission spectroscopy. *Phys. Rev. B*, 60(19):13390, 1999.
- [111] A F Santander-Syro, M Klein, F L Boariu, A Nuber, P Lejay, and F Reinert. Fermi-surface instability at the 'hidden-order' transition of URu<sub>2</sub>Si<sub>2</sub>. *Nat. Phys.*, 5(9):637–641, 2009.
- [112] R Yoshida, Y Nakamura, M Fukui, Y Haga, E Yamamoto, Y Ōnuki, M Okawa, S Shin, M Hirai, Y Muraoka, and *et al.* Signature of hidden order and evidence for periodicity modification in URu<sub>2</sub>Si<sub>2</sub>. *Phys. Rev. B*, 82(20):205108, 2010.
- [113] I Kawasaki, S Fujimori, Y Takeda, T Okane, A Yasui, Y Saitoh, H Yamagami, Y Haga, E Yamamoto, and Y Ōnuki. Electronic structure of URu<sub>2</sub>Si<sub>2</sub> in paramagnetic phase studied by soft x-ray photoemission spectroscopy. *Journal of Physics: Conference Series*, 273(1):012039, 2011.
- [114] G L Dakovski, Y Li, S M Gilbertson, G Rodriguez, A V Balatsky, J-X Zhu, K Gofryk, E D Bauer, P H Tobash, A Taylor, and *et al.* Anomalous femtosecond quasiparticle dynamics of hidden order state in URu<sub>2</sub>Si<sub>2</sub>. *Physical Review B*, 84(16):161103, 2011.
- [115] R Yoshida, M Fukui, Y Haga, E Yamamoto, Y Onuki, M Okawa, W Malaeb, S Shin, Y Muraoka, and T Yokoya. Observation of two fine structures related to the hidden order in the spectral functions of URu<sub>2</sub>Si<sub>2</sub>. *Physical Review B*, 85(24):241102, 2012.
- [116] I Kawasaki, S Fujimori, Y Takeda, T Okane, A Yasui, Y Saitoh, H Yamagami, Y Haga, E Yamamoto, and Y Ōnuki. Band structure and fermi surface of URu<sub>2</sub>Si<sub>2</sub> studied by soft x-ray angle-resolved photoemission spectroscopy. *Physical Review B*, 83(23):235121, 2011.
- [117] F L Boariu, C Bareille, H Schwab, A Nuber, P Lejay, T Durakiewicz, F Reinert, and A F Santander-Syro. Momentum-resolved evolution of the kondo lattice into "hidden order" in URu<sub>2</sub>Si<sub>2</sub>. *Physical Review Letters*, 110(15):156404, 2013.
- [118] S Chatterjee, J Trinckauf, T Hänke, D E Shai, J W Harter, T J Williams, G M Luke, K M Shen, and J Geck. Formation of the coherent heavy fermion liquid at the hidden order transition in URu<sub>2</sub>Si<sub>2</sub>. *Physical Review Letters*, 110(18):186401, 2013.
- [119] R Yoshida, K Tsubota, T Ishiga, M Sunagawa, J Sonoyama, D Aoki, J Flouquet, T Wakita, Y Muraoka, and T Yokoya. Translational symmetry breaking and gapping of heavy-quasiparticle pocket in URu<sub>2</sub>Si<sub>2</sub>. *Scientific reports*, 3(1):1–6, 2013.
- [120] J-Q Meng, P M Oppeneer, J A Mydosh, P S Riseborough, K Gofryk, J J Joyce, E D Bauer, Y Li, and T Durakiewicz. Imaging the three-dimensional fermi-surface pairing near the hidden-order transition in URu<sub>2</sub>Si<sub>2</sub> using angle-resolved photoemission spectroscopy. *Physical Review Letters*, 111(12):127002, 2013.
- [121] C Bareille, F L Boariu, H Schwab, P Lejay, F Reinert, and A F Santander-Syro. Momentum-resolved hidden-order gap reveals symmetry breaking and origin of entropy loss in URu<sub>2</sub>Si<sub>2</sub>. *Nature Communications*, 5(1):1–11, 2014.
- [122] T Durakiewicz. Photoemission investigations of URu<sub>2</sub>Si<sub>2</sub>. *Philosophical Magazine*, 94(32-33):3723–3736, 2014.
- [123] P Ruello, K D Becker, K Ullrich, L Desgranges, C Petot, and G Petot-Ervas. Thermal variation of the optical absorption of UO<sub>2</sub>: determination of the small polaron self-energy. *Journal of nuclear materials*, 328(1):46–54, 2004.
- [124] J G Tobin and S-W Yu. Orbital specificity in the unoccupied states of UO<sub>2</sub> from resonant inverse photoelectron spectroscopy. *Physical Review Letters*, 107(16):167406, 2011.
- [125] S M Gilbertson, T Durakiewicz, G L Dakovski, Y Li, J-X Zhu, S D Conradson, S A Trugman, and G Rodriguez. Ultrafast photoemission spectroscopy of the uranium dioxide UO<sub>2</sub> mott insulator: Evidence for a robust energy gap structure. *Physical Review Letters*, 112(8):087402, 2014.
- [126] L E Roy, T Durakiewicz, R L Martin, J E Peralta, G E Scuseria, C G Olson, J J Joyce, and E Guzewicz. Dispersion in the mott insulator UO<sub>2</sub>: A comparison of photoemission spectroscopy and screened hybrid density functional theory. *Journal of computational chemistry*, 29(13):2288–2294, 2008.
- [127] J J Joyce, A J Arko, L E Cox, and S Czuchlewski. Resonance photoelectron spectroscopy using a tunable laser plasma light source. *Surface and Interface Analysis: An International Journal devoted to the development and application of techniques for the analysis of surfaces, interfaces and thin films*, 26(2):121–123, 1998.
- [128] S L Molodtsov, J Boysen, M Richter, P Segovia, C Laubschat, S A Gorovikov, A M Ionov, G V Prudnikova, and V K Adamchuk. Dispersion of 5f electron states: Angle-resolved photoemission on ordered films of U metal. *Physical Review B*, 57(20):13241, 1998.
- [129] L Berbil-Bautista, T Hänke, M Getzlaff, R Wiesendanger, I Opahle, K Koepf, and M Richter. Observation of 5f states in U/W (110) films by means of scanning tunneling spectroscopy. *Physical Review B*, 70(11):113401, 2004.
- [130] M Zarshenas and S J Asadabadi. Theoretical study of  $\alpha$ -U/W (110) thin films from density functional theory calculations: structural, magnetic and electronic properties. *Thin Solid Films*, 520(7):2901–2908, 2012.
- [131] R Springell, B Detlefs, G H Lander, R C C Ward, R A Cowley, N Ling, W Goetze, R Ahuja, W Luo, and B Johansson. Elemental engineering: Epitaxial uranium thin films. *Physical Review B*, 78(19):193403, 2008.
- [132] C P Opeil, R K Schulze, H M Volz, J C Lashley, M E Manley, W L Hulst, R J Hanrahan Jr, J L Smith, B Mihaila, K B Blagoev, et al. Angle-resolved photoemission and first-principles electronic structure of single-crystalline  $\alpha$ -u (001). *Physical Review B*, 75(4):045120,

- 2007.
- [133] C P Opeil, R K Schulze, M E Manley, J C Lashley, W L Hulst, R J Hanrahan Jr, J L Smith, B Mihaila, K B Blagoev, R C Albers, et al. Valence-band UPS, 6p core-level XPS, and LEED of a uranium (001) single crystal. *Physical Review B*, 73(16):165109, 2006.
- [134] Q Chen, S Tan, W Feng, L Luo, X Zhu, and X Lai. Direct observation of the f-c hybridization in the ordered uranium films on W (110). *Chinese Physics B*, 28(7):077404, 2019.
- [135] J J Joyce, T Durakiewicz, K S Graham, E D Bauer, D P Moore, J N Mitchell, J A Kennison, T M McCleskey, Q Jia, A K Burrell, and et al. 5f electronic structure and fermiology of Pu materials. *MRS Online Proceedings Library*, 1264(1):1–6, 2010.
- [136] R E Jilek, E Bauer, A K Burrell, T M McCleskey, Q Jia, B L Scott, M F Beaux, T Durakiewicz, J J Joyce, K D Rector, and et al. Preparation of epitaxial uranium dicarbide thin films by polymer-assisted deposition. *Chemistry of Materials*, 25(21):4373–4377, 2013.
- [137] S Middlemas, Z Hua, V Chauhan, W T Yorgason, R Schley, A Khanolkar, M Khafizov, and D Hurley. Determining local thermal transport in a composite uranium-nitride/silicite nuclear fuel using square-pulse transient thermoreflectance technique. *Journal of Nuclear Materials*, 528:151842, 2020.
- [138] M Sanati, R C Albers, T Lookman, and A Saxena. Elastic constants, phonon density of states, and thermal properties of UO<sub>2</sub>. *Physical Review B*, 84(1):014116, 2011.
- [139] P Santini, S Carretta, G Amoretti, R Caciuffo, N Magnani, and G H Lander. Multipolar interactions in f-electron systems: The paradigm of actinide dioxides. *Reviews of Modern Physics*, 81(2):807, 2009.
- [140] N Magnani, P Santini, G Amoretti, and R Caciuffo. Perturbative approach to j mixing in f-electron systems: Application to actinide dioxides. *Physical Review B*, 71(5):054405, 2005.
- [141] M Mann, D Thompson, K Serivalsatit, T M Tritt, J Balato, and J Kolis. Hydrothermal growth and thermal property characterization of ThO<sub>2</sub> single crystals. *Crystal growth & design*, 10(5):2146–2151, 2010.
- [142] K Gofryk, S Du, C R Stanek, J C Lashley, X-Y Liu, R K Schulze, J L Smith, D J Safarik, D D Byler, K J McClellan, and et al. Anisotropic thermal conductivity in uranium dioxide. *Nature communications*, 5(1):1–7, 2014.
- [143] T Nishi, A Itoh, M Takano, M Numata, M Akabori, Y Arai, and K Minato. Thermal conductivity of neptunium dioxide. *Journal of nuclear materials*, 376(1):78–82, 2008.
- [144] J F Lagedrost, D F Askey, V W Storhok, and J E Gates. Thermal conductivity of PuO<sub>2</sub> as determined from thermal diffusivity measurements. *Nuclear Applications*, 4(1):54–61, 1968.
- [145] S S Parker, J T White, P Hosemann, and A T Nelson. Thermophysical properties of thorium mononitride from 298 to 1700 K. *Journal of Nuclear Materials*, 526:151760, 2019.
- [146] M Khafizov, V Chauhan, Y Wang, F Riyad, N Hang, and D H Hurley. Investigation of thermal transport in composites and ion beam irradiated materials for nuclear energy applications. *Journal of Materials Research*, 32(1):204–216, 2017.
- [147] M N Luckyanova, J A Johnson, A A Maznev, J Garg, A Jandi, M T Bulsara, E A Fitzgerald, K A Nelson, and G Chen. Anisotropy of the thermal conductivity in GaAs/AlAs superlattices. *Nano Lett.*, 13:3973–3977, 2013.
- [148] A Giri, J L Braun, and P E Hopkins. Effect of crystalline/amorphous interfaces on thermal transport across confined thin films and superlattices. *Journal of Applied Physics*, 119(23):235305, 2016.
- [149] P Santini, R Lemanski, and P Erdős. Magnetism of actinide compounds. *Advances in Physics*, 48(5):537–653, 1999.
- [150] G J-P Deblonde, M Zavarin, and A B Kersting. The coordination properties and ionic radius of actinium: A 120-year-old enigma. *Coordination Chemistry Reviews*, 446:214130, 2021.
- [151] L Severin, M S S Brooks, and B Johansson. Relationship between the Coulomb integral  $U$  and the stoner parameter  $I$ . *Physical Review Letters*, 71(19):3214, 1993.
- [152] J C Lashley, A Lawson, R J McQueeney, and G H Lander. Absence of magnetic moments in plutonium. *Physical Review B*, 72(5):054416, 2005.
- [153] M Janoschek, P Das, B Chakrabarti, D L Abernathy, M D Lumsden, J M Lawrence, J D Thompson, G H Lander, J N Mitchell, S Richmond, and et al. The valence-fluctuating ground state of plutonium. *Science Advances*, 1(6):e1500188, 2015.
- [154] G H Lander, J-C Griveau, R Eloirdi, N Magnani, E Colineau, F Wilhelm, SD Brown, D Wermeille, A Rogalev, RG Haire, and et al. Measurements related to the magnetism of curium metal. *Physical Review B*, 99(22):224419, 2019.
- [155] H R Ott, Z Fisk, A J Freeman, and G H Lander. Handbook on the physics and chemistry of the actinides. *AJ Freeman, GH Lander, Noth-Holland, Amsterdam*, pages 85–225, 1987.
- [156] M Marutzky, U Barkow, J Schoenes, and R Troć. Optical and magneto-optical properties of single crystalline uranium nitride. *Journal of magnetism and magnetic materials*, 299(1):225–230, 2006.
- [157] H Sakai, H Kato, Y Tokunaga, S Kambe, R E Walstedt, A Nakamura, N Tateiwa, and T C Kobayashi. Magnetism of uranium dioxide UO<sub>2</sub> under high pressure. *Journal of Magnetism and Magnetic Materials*, 272:E413–E414, 2004.
- [158] V Ichas, S Zwirner, D Braithwaite, J C Spirlet, J Rebizant, and W Potzel. Electrical resistance and magnetic properties of the neptunium mononitrides NpAs, NpSb, and NpBi at high pressures. *Physical Review B*, 56(22):14481, 1997.
- [159] S E Nave, R G Haire, and P G Huray. Magnetic properties of actinide elements having the 5f<sup>6</sup> and 5f<sup>7</sup> electronic configurations. *Physical Review B*, 28(5):2317, 1983.
- [160] M Jin, Y Guo, B Li, X Niu, and Y Zhang. Magnetic and electronic properties of  $\alpha$ -U<sub>2</sub>N<sub>3</sub> and its role in preventing uranium from oxidation: First-principles studies. *Journal of Nuclear Materials*, 512:72–78, 2018.
- [161] E L Bright, R Springell, D G Porter, S P Collins, and G H Lander. Synchrotron x-ray scattering of magnetic and electronic structure of UN and U<sub>2</sub>N<sub>3</sub> epitaxial films. *Physical Review B*, 100(13):134426, 2019.
- [162] K Shrestha, D Antonio, M Jaime, N Harrison, D S Mast, D Safarik, T Durakiewicz, J-C Griveau, and

- K Gofryk. Tricritical point from high-field magnetoelastic and metamagnetic effects in UN. *Scientific Reports*, 7(1):1–8, 2017.
- [163] R Troć, M Samsel-Czekala, A Pikul, A V Andreev, D I Gorbunov, Y Skourski, and J Sznajd. Electronic structure of UN based on specific heat and field-induced transitions up to 65 T. *Physical Review B*, 94(22):224415, 2016.
- [164] S Hamann, T Förster, D I Gorbunov, M König, M Uhlarz, J Wosnitza, and T Helm. Fermi-surface reconstruction at the metamagnetic high-field transition in uranium mononitride. *Physical Review B*, 104(15):155123, 2021.
- [165] N M Wolcott and R A Hein. Superconductivity of thorium below 1° K. *Philosophical Magazine*, 3(30):591–596, 1958.
- [166] R D Fowler, B T Matthias, L B Asprey, H H Hill, J D G Lindsay, C E Olsen, and R W White. Superconductivity of protactinium. *Physical Review Letters*, 15(22):860, 1965.
- [167] J L Smith, J C Spirlet, and W Müller. Superconducting properties of protactinium. *Science*, 205(4402):188–190, 1979.
- [168] V G Aschermann and E Justi. Elektrische leitfähigkeit, magnetische widerstandsvermehrung. *Hall-effekt und Supraleitung von Rhenium*, *Phys*, 43:207, 1942.
- [169] B B Goodman and D Shoenberg. Superconductivity of uranium. *Nature*, 165(4194):441–442, 1950.
- [170] J E Gordon, H Montgomery, R J Noer, G R Pickett, and R Tobón. Superconductivity of thorium and uranium. *Physical Review*, 152(1):432, 1966.
- [171] Kevin T Moore and Gerrit van der Laan. Nature of the 5 f states in actinide metals. *Reviews of Modern Physics*, 81(1):235, 2009.
- [172] J L Smith and R G Haire. Superconductivity of americium. *Science*, 200(4341):535–537, 1978.
- [173] J-C Griveau and E Colineau. Superconductivity in transuranium elements and compounds. *Comptes Rendus Physique*, 15(7):599–615, 2014.
- [174] M B Maple, M C de Andrade, J Herrmann, R P Dickey, N R Dilley, and S Han. Superconductivity in rare earth and actinide compounds. *Journal of alloys and compounds*, 250(1-2):585–595, 1997.
- [175] D Aoki, Y Haga, T D Matsuda, N Tateiwa, S Ikeda, Y Homma, H Sakai, Y Shiokawa, E Yamamoto, A Nakamura, and *et al.* Unconventional heavy-fermion superconductivity of a new transuranium compound NpPd<sub>5</sub>Al<sub>2</sub>. *Journal of the Physical Society of Japan*, 76(6):063701, 2007.
- [176] J-C Griveau, K Gofryk, and J Rebizant. Transport and magnetic properties of the superconductor NpPd<sub>5</sub>Al<sub>2</sub>. *Physical Review B*, 77(21):212502, 2008.
- [177] E D Bauer, M M Altarawneh, P H Tobash, K Gofryk, O E Ayala-Valenzuela, J N Mitchell, R D McDonald, C H Mielke, F Ronning, J C Griveau, and *et al.* Localized 5f electrons in superconducting PuCoIn<sub>5</sub>: consequences for superconductivity in PuCoGa<sub>5</sub>. *Journal of Physics: Condensed Matter*, 24(5):052206, 2011.
- [178] F Wastin, P Boulet, J Rebizant, E Colineau, and GH Lander. Advances in the preparation and characterization of transuranium systems. *Journal of Physics: Condensed Matter*, 15(28):S2279, 2003.
- [179] E D Bauer and J D Thompson. Plutonium-based heavy-fermion systems. *Annu. Rev. Condens. Matter Phys.*, 6(1):137–153, 2015.
- [180] H R Ott, H Rudigier, Z Fisk, and J L Smith. UBe<sub>13</sub>: An unconventional actinide superconductor. *Physical review letters*, 50(20):1595, 1983.
- [181] B J Ramshaw, A Shekhter, R D McDonald, J B Betts, J N Mitchell, P H Tobash, C H Mielke, E D Bauer, and A Migliori. Avoided valence transition in a plutonium superconductor. *Proceedings of the National Academy of Sciences*, 112(11):3285–3289, 2015.
- [182] K Gofryk, J-C Griveau, P S Riseborough, and T Durakiewicz. Thermoelectric power as a probe of density of states in correlated actinide materials: The case of PuCoGa<sub>5</sub> superconductor. *Physical Review B*, 94(19):195117, 2016.
- [183] S Ran, C Eckberg, Q-P Ding, Y Furukawa, T Metz, S R Saha, I-L Liu, M Zic, H Kim, J Paglione, and *et al.* Nearly ferromagnetic spin-triplet superconductivity. *Science*, 365(6454):684–687, 2019.
- [184] G Nakamine, S Kitagawa, K Ishida, Y Tokunaga, H Sakai, S Kambe, A Nakamura, Y Shimizu, Y Homma, D Li, and *et al.* Superconducting properties of heavy fermion UTe<sub>2</sub> revealed by <sup>125</sup>Te-nuclear magnetic resonance. *journal of the physical society of japan*, 88(11):113703, 2019.
- [185] D Braithwaite, M Vališka, G Knebel, G Lapertot, J-P Brison, A Pourret, ME Zhitomirsky, J Flouquet, F Honda, and D Aoki. Multiple superconducting phases in a nearly ferromagnetic system. *Communications Physics*, 2(1):1–6, 2019.
- [186] I M Hayes, D S Wei, T Metz, J Zhang, Y S Eo, S Ran, S R Saha, J Collini, N P Butch, D F Agterberg, and *et al.* Weyl superconductivity in UTe<sub>2</sub>. *arXiv preprint arXiv:2002.02539*, 2020.
- [187] S Bae, H Kim, Y S Eo, S Ran, I Liu, W T Fuhrman, J Paglione, N P Butch, S M Anlage, and *et al.* Anomalous normal fluid response in a chiral superconductor UTe<sub>2</sub>. *Nature communications*, 12(1):1–5, 2021.
- [188] C Brun, T Cren, and D Roditchev. Review of 2D superconductivity: the ultimate case of epitaxial monolayers. *Superconductor Science and Technology*, 30(1):013003, 2016.
- [189] V Bhardwaj, A Bhattacharya, L K Varga, A K Ganguli, and R Chatterjee. Thickness-dependent magnetotransport properties of topologically nontrivial DyPdBi thin films. *Nanotechnology*, 31(38):384001, 2020.
- [190] A Cossard, J K Desmarais, S Casassa, C Gatti, and A Erba. Charge density analysis of actinide compounds from the quantum theory of atoms in molecules and crystals. *The journal of physical chemistry letters*, 12(7):1862–1868, 2021.
- [191] P Richmond and G L Sewell. Electron correlations, magnetic ordering, and mott insulation in solids. *Journal of Mathematical Physics*, 9(3):349–356, 1968.
- [192] J Krumrain, G Mussler, S Borisova, T Stoica, L Plucinski, CM Schneider, and D Grützmacher. Mbe growth optimization of topological insulator Bi<sub>2</sub>Te<sub>3</sub> films. *Journal of Crystal Growth*, 324(1):115–118, 2011.
- [193] S Tang, C Zhang, D Wong, Z Pedramrazi, H-Z Tsai, C Jia, B Moritz, M Claassen, H Ryu, S Kahn, and *et al.* Quantum spin hall state in monolayer 1T'-WTe<sub>2</sub>. *Nature Physics*, 13(7):683–687, 2017.
- [194] T Hesjedal. Rare earth doping of topological insulators: A brief review of thin film and heterostructure systems. *physica status solidi (a)*, 216(8):1800726, 2019.

- [195] V Ivanov, X Wan, and S Y Savrasov. Topological insulator-to-weyl semimetal transition in strongly correlated actinide system UNiSn. *Physical Review X*, 9(4):041055, 2019.
- [196] X Zhang, H Zhang, J Wang, C Felser, and S-C Zhang. Actinide topological insulator materials with strong interaction. *Science*, 335(6075):1464–1466, 2012.
- [197] H Choi, W Zhu, S K Cary, L E Winter, Z Huang, R D McDonald, V Mocko, B L Scott, P H Tobash, J D Thompson, and *et al.* Experimental and theoretical study of topology and electronic correlations in PuB<sub>4</sub>. *Physical Review B*, 97(20):201114, 2018.
- [198] A P Dioguardi, H Yasuoka, S M Thomas, H Sakai, S K Cary, S A Kozimor, T E Albrecht-Schmitt, H C Choi, J-X Zhu, J D Thompson, and *et al.* <sup>239</sup>Pu nuclear magnetic resonance in the candidate topological insulator PuB<sub>4</sub>. *Physical Review B*, 99(3):035104, 2019.
- [199] X Deng, K Haule, and G Kotliar. Plutonium hexaboride is a correlated topological insulator. *Physical review letters*, 111(17):176404, 2013.
- [200] M Dzero, K Sun, V Galitski, and P Coleman. Topological Kondo insulators. *Physical review letters*, 104(10):106408, 2010.
- [201] W Kohn and L J Sham. Self-consistent equations including exchange and correlation effects. *Physical Review*, 140:1133, 1965.
- [202] P Hohenberg and W Kohn. Inhomogeneous electron gas. *Phys. Rev.*, 136:864, 1964.
- [203] K Burke. Perspective on density functional theory. *Journal Of Chemical Physics*, 136:150901, 2012.
- [204] R O Jones. Density functional theory: its origins, rise to prominence, and future. *Rev. Mod. Phys.*, 87:897, 2015.
- [205] C J Cramer and D G Truhlar. Density functional theory for transition metals and transition metal chemistry. *Physical Chemistry Chemical Physics*, 11:10757, 2009.
- [206] P J Hasnip, K Refson, M Probert, J R Yates, S J Clark, and C J Pickard. Density functional theory in the solid state. *Philosophical Transactions Of The Royal Society A-mathematical Physical And Engineering Sciences*, 372:20130270, 2014.
- [207] A Jain, Y Shin, and K A Persson. Computational predictions of energy materials using density functional theory. *Nature Reviews Materials*, 1:15004, 2016.
- [208] R J Maurer, C Freysoldt, A M Reilly, J G Brandenburg, O T Hofmann, T Bjorkman, S Lebegue, and A Tkatchenko. Advances in density-functional calculations for materials modeling. *Annual Review Of Materials Research, Vol 49 Se Annual Review Of Materials Research*, 49:1, 2019.
- [209] J P Perdew and K Schmidt. Jacob’s ladder of density functional approximations for the exchange-correlation energy. *Density Functional Theory And Its Application To Materials*, edited by V. Van Doren, C. Van Alsenoy, and P. Geerlings, 577:1, 2001.
- [210] G Kotliar, S Y Savrasov, K Haule, V S Oudovenko, O Parcollet, and C A Marianetti. Electronic structure calculations with dynamical mean-field theory. *Rev. Mod. Phys.*, 78:865, 2006.
- [211] A J Cohen, P Mori-Sanchez, and W T Yang. Insights into current limitations of density functional theory. *Science*, 321:792, 2008.
- [212] M Imada, A Fujimori, and Y Tokura. Metal-insulator transitions. *Rev. Mod. Phys.*, 70:1039, 1998.
- [213] J P Perdew, W T Yang, K Burke, Z H Yang, E Gross, M Scheffler, G E Scuseria, T M Henderson, I Y Zhang, A Ruzsinszky, and *et al.* Understanding band gaps of solids in generalized Kohn-Sham theory. *Proceedings Of The National Academy Of Sciences Of The United States Of America*, 114:2801, 2017.
- [214] A Georges, G Kotliar, W Krauth, and M J Rozenberg. Dynamical mean-field theory of strongly correlated fermion systems and the limit of infinite dimensions. *Rev. Mod. Phys.*, 68:13, 1996.
- [215] P Werner, A Comanac, L D Medici, M Troyer, and A J Millis. Continuous-time solver for quantum impurity models. *Phys. Rev. Lett.*, 97:076405, 2006.
- [216] K Haule. Quantum monte carlo impurity solver for cluster dynamical mean-field theory and electronic structure calculations with adjustable cluster base. *Phys. Rev. B*, 75:155113, 2007.
- [217] E Gull, A J. Millis, A I. Lichtenstein, A N. Rubtsov, M Troyer, and P Werner. Continuous-time monte-carlo methods for quantum impurity models. *Rev. Mod. Phys.*, 83:349, May 2011.
- [218] C A Marianetti, K Haule, G Kotliar, and M J Fluss. Electronic coherence in delta-Pu: a dynamical mean-field theory study. *Phys. Rev. Lett.*, 101:056403, 2008.
- [219] H Park, A J Millis, and C A Marianetti. Total energy calculations using DFT plus DMFT: computing the pressure phase diagram of the rare earth nickelates. *Phys. Rev. B*, 89:245133, 2014.
- [220] E B Isaacs and C A Marianetti. Compositional phase stability of correlated electron materials within DFT+DMFT. *Phys. Rev. B*, 102:045146, Jul 2020.
- [221] R Adler, C J Kang, C H Yee, and G Kotliar. Correlated materials design: prospects and challenges. *Reports On Progress In Physics*, 82:012504, 2019.
- [222] B Chakrabarti, T Birol, and K Haule. Role of entropy and structural parameters in the spin-state transition of LaCoO<sub>3</sub>. *Physical Review Materials*, 1:064403, 2017.
- [223] F Lechermann. Multiorbital processes rule the Nd<sub>1-x</sub>Sr<sub>x</sub>NiO<sub>2</sub> normal state. *Physical Review X*, 10:041002, 2020.
- [224] V I Anisimov, F Aryasetiawan, and A I Lichtenstein. First-principles calculations of the electronic structure and spectra of strongly correlated systems: the LDA+U method. *Journal Of Physics-condensed Matter*, 9:767, 1997.
- [225] B D Sahoo, K D Joshi, and T C Kaushik. Structural, elastic, vibrational, thermophysical properties and pressure-induced phase transitions of ThN<sub>2</sub>, Th<sub>2</sub>N<sub>3</sub>, and Th<sub>3</sub>N<sub>4</sub>: An ab initio investigation. *Journal of Applied Physics*, 128(3):035902, 2020.
- [226] J Adachi, K Kurosaki, M Uno, and S Yamanaka. A molecular dynamics study of thorium nitride. *Journal of alloys and compounds*, 394(1-2):312–316, 2005.
- [227] R Atta-Fynn and Asok K Ray. Density functional study of the actinide nitrides. *Physical Review B*, 76(11):115101, 2007.
- [228] N Reyren, S Thiel, A D Caviglia, L F Kourkoutis, G Hammerl, C Richter, C W Schneider, T Kopp, A S Ruetschi, D Jaccard, M Gabay, D A Muller, J M Triscone, and J Mannhart. Superconducting interfaces between insulating oxides. *Science*, 317:1196, 2007.
- [229] D D Castro, C Cantoni, F Ridolfi, C Aruta, A Tebano, N Yang, and G Balestrino. High-T<sub>c</sub> superconductivity at the interface between the CaCuO<sub>2</sub> and SrTiO<sub>3</sub> insu-

- lating oxides. *Phys. Rev. Lett.*, 115:147001, 2015.
- [230] U Luders, W C Sheets, A David, W Prellier, and R Fressard. Room-temperature magnetism in  $\text{LaVO}_3/\text{SrVO}_3$  superlattices by geometrically confined doping. *Phys. Rev. B*, 80:241102, 2009.
- [231] A V Boris, Y Matiks, E Benckiser, A Frano, P Popovich, V Hinkov, P Wochner, M Castro-colin, E Detemple, V K Malik, C Bernhard, T Prokscha, A Suter, Z Salman, E Morenzoni, G Cristiani, H U Habermeier, and B Keimer. Dimensionality control of electronic phase transitions in nickel-oxide superlattices. *Science*, 332:937, 2011.
- [232] J Chakhalian, J W Freeland, H U Habermeier, G Cristiani, G Khaliullin, M VanVeenendaal, and B Keimer. Orbital reconstruction and covalent bonding at an oxide interface. *Science*, 318:1114, 2007.
- [233] M Bibes, J E Villegas, and A Barthelemy. Ultrathin oxide films and interfaces for electronics and spintronics. *Advances In Physics*, 60:5, 2011.
- [234] H H Chen, A J Millis, and C A Marianetti. Engineering correlation effects via artificially designed oxide superlattices. *Phys. Rev. Lett.*, 111:116403, 2013.
- [235] Z C Zhong, M Wallerberger, J M Tomczak, C Taranto, N Parragh, A Toschi, G Sangiovanni, and K Held. Electronics with correlated oxides:  $\text{SrVO}_3/\text{SrTiO}_3$  as a Mott transistor. *Phys. Rev. Lett.*, 114:246401, 2015.
- [236] A James, M Aichhorn, and J Laverock. Quantum confinement induced metal-insulator transition in strongly correlated quantum wells of  $\text{SrVO}_3$  superlattices. *Physical Review Research*, 3:023149, 2021.
- [237] D Gao and A K Ray. On the convergence of the electronic structure properties of the fcc americium (0 0 1) surface. *Surface science*, 600(22):4941–4952, 2006.
- [238] D Gao and A K Ray. Relativistic density functional study of fcc americium and the (111) surface. *Physical Review B*, 77(3):035123, 2008.
- [239] E L Sikorski, B J Jaques, and L Li. First-principles magnetic treatment of the uranium nitride (100) surface and effect on corrosion initiation. *Journal of Applied Physics*, 130(9):095301, 2021.
- [240] H Kroemer. Quasi-electric fields and band offsets: Teaching electrons new tricks (nobel lecture). *ChemPhysChem*, 2(8-9):490–499, 2001.
- [241] C A Dennett, N Poudel, P J Simmonds, A Tiwari, D H Hurley, and K Gofryk. Towards actinide heterostructure synthesis and science. *Nat. Commun.*, 2022. Accepted.
- [242] M Block, M Laatiaoui, and S Raeder. Recent progress in laser spectroscopy of the actinides. *Progress in Particle and Nuclear Physics*, 116:103834, 2021.
- [243] P Grover, L S Ferch, and G Schreckenbach. Adsorption of actinide (U–Pu) complexes on the silicene and germanene surface: A theoretical study. *The Journal of Physical Chemistry A*, 124(8):1522–1534, 2020.
- [244] A Lopez-Bezanilla. f-orbital based Dirac states in a two-dimensional uranium compound. *Journal of Physics: Materials*, 3(2):024002, 2020.
- [245] S-J Park and M-K Seo. *Interface science and composites*, volume 18. Academic Press, 2011.
- [246] S Murali, C Zhang, M Goryll, R R King, and C B Honsberg. Study of pit formation in MBE grown GaP on mis-oriented Si. *Journal of Vacuum Science & Technology B, Nanotechnology and Microelectronics: Materials, Processing, Measurement, and Phenomena*, 38(3):032201, 2020.
- [247] J Simon, S Tomasulo, P J Simmonds, M Romero, and M L Lee. Metamorphic gaasp buffers for growth of wide-bandgap ingap solar cells. *Journal of Applied Physics*, 109:013708, 2011.
- [248] D Benyahia, L Kubiszyn, K Michalczewski, A Kęłowski, P Martyniuk, J Piotrowski, A Rogalski, and *et al.* Optimization of the interfacial misfit array growth mode of GaSb epilayers on GaAs substrate. *Journal of Crystal Growth*, 483:26–30, 2018.
- [249] K E Sautter, K D Vallejo, and P J Simmonds. Strain-driven quantum dot self-assembly by molecular beam epitaxy. *Journal of Applied Physics*, 128(3):031101, 2020.
- [250] T Makimoto, K Kumakura, M Maeda, H Yamamoto, and Y Horikoshi. A new AlON buffer layer for RF-MBE growth of AlN on a sapphire substrate. *Journal of Crystal Growth*, 425:138–140, 2015.
- [251] K D Vallejo, T A Garrett, C I Cabrera, B Liang, K A Grossklaus, and P J Simmonds. Tensile-strained self-assembly of InGaAs on InAs (111) a. *Journal of Vacuum Science & Technology B, Nanotechnology and Microelectronics: Materials, Processing, Measurement, and Phenomena*, 39(6):062809, 2021.
- [252] X He, Y Feng, X Yang, S Wu, Z Cai, J Wei, J Shen, H Huang, D Liu, Z Chen, and *et al.* Step-graded Al-GaN vs superlattice: role of strain relief layer in dynamic on-resistance degradation. *Applied Physics Express*, 15(1):011001, 2021.
- [253] U Nandi, M Mohammadi, H Lu, J Norman, A C Gosard, L Alff, and S Preu. Material properties and performance of ErAs: In(Al)GaAs photoconductors for 1550 nm laser operation. *Journal of Vacuum Science & Technology A: Vacuum, Surfaces, and Films*, 39(2):023407, 2021.
- [254] P Jin, X L Ye, and Z G Wang. Growth of low-density InAs/GaAs quantum dots on a substrate with an intentional temperature gradient by molecular beam epitaxy. *Nanotechnology*, 16(12):2775, 2005.
- [255] J W Matthews and A E Blakeslee. Defects in epitaxial multilayers: I. misfit dislocations. *Journal of Crystal growth*, 27:118–125, 1974.
- [256] F A Rough and A A Bauer. Constitution of uranium and thorium alloys. Technical report, Battelle Memorial Inst., Columbus, Ohio, 1958.